MODELLING AND SIMULATION OF A DOUBLY-FED INDUCTION GENERATOR BASED WIND TURBINE UNDER SYMMETRICAL VOLTAGE FAULT

A Thesis Submitted to
the Graduate School of Engineering and Sciences of
İzmir Institute of Technology
in Partial Fulfillment of the Requirements for the Degree of

MASTER OF SCIENCE

in Energy Engineering

by
Elif Dilara ÇİÇEK

October 2023
İZMİR

We approve the thesis of **Elif Dilara ÇİÇEK.**

Examining Committee Members:

Prof. Dr. Gülden Gökçen AKKURT
Department of Energy Engineering, Izmir Institute of Technology

Assoc. Prof. Dr. Taner GÖKTAŞ
Department of Electrical-Electronics Engineering, Dokuz Eylul University

Assoc. Prof. Erhan DEMİROK
Department of Electrical-Electronics Engineering, Katip Celebi University

11/October/2023

Prof. Dr. Gülden Gökçen AKKURT
Supervisor, Department of Energy Engineering
Izmir Institute of Technology

Assoc. Prof. Kerem ALTUN
Co-Supervisor, Department of Mechanical Engineering
Isik University

Prof. Dr. Gülden Gökçen AKKURT
Head of the Department of Energy Engineering

Prof. Mehtap EANES
Dean of the Graduate School of Engineering and Science

ACKNOWLEDGEMENTS

First and foremost, I would like to express my heartfelt gratitude to my advisors, Prof. Dr. Gülden Gökçen AKKURT and Asst. Prof. Dr. Kerem ALTUN, for their invaluable advice and support throughout my thesis.

I am grateful for the support of my family: my father, Mehmet ÇİÇEK and my mother, Nafiye ÇİÇEK, as well as all my sisters and brother. I would also like to extend my gratitude to my nephews, whose presence I missed throughout the entire working process. Their motivation served as a source of inspiration for me. I express my heartfelt appreciation for your unwavering presence and support.

Lastly, I would like to thank a very special person, Bora DOĞAROĞLU, for his kind support during my thesis study.

ABSTRACT

MODELLING AND SIMULATION OF A DOUBLY-FED INDUCTION GENERATOR BASED WIND TURBINE UNDER SYMMETRICAL VOLTAGE FAULT

When wind turbines, which convert wind energy, one of the renewable energy sources, into electrical energy, are connected to the electrical grid, it is of great importance to maintain grid stability. However, the variable nature of wind can pose certain challenges to system stability in wind turbine grid integration. Regulations in different countries require wind turbines to continue contributing to the grid in the event of a fault. In this thesis, the process of converting wind energy into electrical energy through a specific generator is described, and the behaviour of the turbine is simulated in the event of a symmetrical voltage fault.

This thesis aims to develop a simulation model for a variable-speed doubly fed asynchronous generator-based (Dfig) wind turbine with a partially scaled frequency converter control using the field-oriented vector control method and to investigate its grid contribution ability under different conditions. The aim was to ensure torque control on the generator side and grid-side control. After the completion of the control system, the turbine's grid contribution ability was examined under short-term faults, and it has been shown that the system continues to contribute to the grid after the voltage drop. The modelling was performed using the Matlab / Simulink program, and the results were shared. In the last part of the thesis, the effect of a symmetrical fault on the rotor current is analysed by the Monte Carlo method.

ÖZET

ÇİFT BESLEMELİ ASENKRON JENERATÖR TABANLI RÜZGAR TÜRBİNİNİN SİMETRİK GERİLİM ARIZASI ALTINDA MODELLENMESİ VE SİMÜLASYONU

Dünya genelinde artan enerji penetrasyonu ile rüzgâr enerjisi fosil yakıtlara, yüksek elektrik üretim kapasitesi ile güçlü bir alternatif oluşturmaktadır. Rüzgârdan sağlanan enerjinin mekaniksel ve elektriksel bileşenler aracılığıyla elektrik enerjisine dönüştürüldüğü sistemler olan rüzgâr türbinleri, şebekeye bağlandığında şebeke sistemi kararlılığının korunması önem arz etmektedir. Rüzgârın değişken yapısı, türbinlerin şebeke bağlantısında sistem kararlılığı bakımından bazı problemlere neden olabilmektedir. Ülkeler özelinde yönetmeliklerde, rüzgâr türbinlerinin olası bir arıza anında sisteme katkı sağlamaya devam etmesi zorunluluğu mevcuttur. Bu tez çalışmasında, modellenen jeneratör ile olası bir simetrik voltaj arızası anında, türbinin davranışı simüle edilmiştir.

Değişken hızlı, Çift Beslemeli Asenkron Jeneratörlü bir rüzgâr türbini için kısmi ölçekli frekans dönüştürücü kontrolünün alan yönlendirmeli vektör kontrol yöntemi ile simülasyon modelinin oluşturulması ve farklı koşullar altında şebeke sistemine katkı yeteneğinin incelenmesi amaçlanmıştır. Tez çalışmasının amacı doğrultusunda, çift beslemeli asenkron jeneratörlü bir rüzgâr türbininin matematiksel modellemesi yapılmıştır. Dönüştürücünün jeneratör tarafı ile tork kontrolünün sağlanması ve şebeke tarafı ile DC bağlantısının kontrol altında tutulması amaçlanmıştır. Kontrol sistemi tamamlandıktan sonra şebekede oluşturulan kısa süreli arıza ile türbinin arıza sonrası şebeke sistemine katkı yeteneği incelenmiş ve voltaj düşüşü sonrasında sistemin şebekeye katkı sağlamaya devam ettiği gösterilmiştir. Modelleme, Matlab / Simulink programı ile yapılmış ve sonuçları paylaşılmıştır. Tezin son bölümünde asimetrik arızanın rotor akımı üzerindeki etkisini incelemek amacıyla simülasyonda farklı gerilim düşüşleri oluşturulmuş ve Monte Carlo yöntemi ile analiz edilmiştir.

TABLE OF CONTENTS

LIST OF FIGURES

Figure **Page**

LIST OF TABLES

Table **Page**

ABBREVIATIONS

BEM	: Main Element Momentum
DFIG	: Doubly Fed Induction Generator
DVR	: Dynamic Voltage Restorer
EMT	: Electromagnetic transient
ENTSO-E	: European Grid of Transmission System Operators for Electricity
FLL	: Frequency Locked Loop
FRT	: Fault Ride Through
FSWT	: Fixed Speed Wind Turbines
GSC	: Grid Side Converter
IEC	: International Electrotechnical Commission
IGBTs	: Insulated Gate Bipolar Transistors
LVRT	: Low Voltage Ride Through
MPC	: Model Base Control
MPPT	: Maximum Power Point Tracker
PCC	: Point of Common Coupling
PLL	: Phase Lock Loop
PMSG	: Permanent Magnet Synchronous Generator
PWM	: Pulse Width Modulation
RCI	: Reactive Current Injection
RMS	: Root Mean Square
RSC	: Rotor Side Converter
SCIG	: Squirrel Cage Induction Generator
SMC	: Sliding Mode Control
STATCOM	: Static Synchronous Compensator
VSC	: Voltage Side Control
VSS	: Variable Structural Systems
VSWT	: Variable Speed Wind Turbines
WECS	: Wind Energy Conversion Systems
WPPs	: Wind Power Plants
WRIG	: Wound-Rotor Induction Generator
WRSG	: Wound-Rotor Synchronous Generator

LIST OF SYMBOLS

$L^{\sigma s}$: Stator leakage inductance (H)

$L^{\sigma r}$: Rotor leakage inductance (H)

L^{m} : Mutual inductance (H)

R^{s} : Stator resistance (Ω)

R^{r} : Rotor resistance (Ω)

L^{sr} : Amplitude of the inductance matrix

θ_r : Instantaneous angle difference between stator and rotor axes

Ns, Nr : Number of turns per phase for stator and rotor windings.

ψ_s : Stator flux

ψ_r : Rotor flux

v^{s}_{abc} : 3 phase supplied stator voltage.

v^{r}_{abc} : 3 phase supplied rotor voltage.

i^{s}_{abc} : 3 phase stators current

i^{r}_{abc} : 3 phase rotors current

T_e : Electromagnetic torque

T_m : Mechanical torque

J : Inertia

B : Magnetic flux density

K^{s} : Krause transforms for stator.

K^{r} : Krause transforms for rotor.

$P_{turbine}$: Turbine power

ρ : Air density (kg/ m^3)

A : Cross-sectional area

C_p : Power conversion coefficient

λ : Tip speed ratio

v^3 : Wind speed (m/s)

ω_{mr} : Rotor angular speed(rad/s) and (m)

Q_s : Stator reactive power

K_Q : Krause transforms for reactive power.

F : Stator frequency (Hz)

Ps	: Rated stator power (W)
n	: Rated rotational speed (rev/min)
Vs	: Rated stator voltage(V)
Is	: Rated stator current(A)
Tem	: Rated torque (N.m)
p	: Pole pair
u	: Stator rotor current turns ratio
Vr	: Rated rotor voltage (V)
smax	: Max slip
Vr_stator	: Rated rotor voltage referred to the stator(V)
Rs	: Stator resistance (ohm)
Lsi	: Leakege inductance (stator-rotor) (H)
Lm	: Magnetizing inductance (H)
Rr	: Rotor resistance referred to stator(ohm)
Ls	: Stator inductance(H)
Lr	: Rotor inductance(H)
Vbus	: DC bus voltage referred to the stator(V)
Fs	: Stator flux (Wb)
J	: Inertia
N	: Gearbox ratio
Cbus	: Dc bus capacitance
Rg	: Grid side filters reference
Lg	: Grid side filters inductance
Rcrowbar	: Crowbar resistance

CHAPTER 1

INTRODUCTION

Wind power generation is constantly evolving globally, and the operation of the grid has become an important component in most countries that have invested heavily in this area. The annual growth of wind power generation worldwide is increasing its impact on the power system and its contribution to the overall energy supply. Countries' clean energy transition policies and legislation are contributing to more wind energy projects in the future, but grid connection of wind farms with high installed power seems to be a major problem. The short-circuit power of the busbar to which the power plant will be connected, the grid impedance angle, the wind turbine characteristics and the generator technology are also decisive factors in the integration of wind power plants with the grid. The grid legislation is primarily focused on supporting reactive power to tackle the voltage stability problem in both the steady and transient regimes. The regulations obligate that power plants continue to generate active electricity and inject reactive power into the grid during a voltage drop that occurs at the point where the wind farms are connected to the system in order to remove the voltage drop urgently.

The literature review about the thesis topic is briefly discussed in this part. The literature studies focus on modelling and approach for faults that may occur when a doubly fed asynchronous generator (DFIG) based wind turbine is connected to the grid. The primary purpose of the DFIG is to keep on running during fault. Matlab / Simulink program was used for the model to be utilized in the study. The interest in green energy resources is increasing daily in the modern world with the growing energy demand. The wind is among the most critical types of energy for our electrical resources. The opportunity to work with environmentally friendly, sustainable, and high powers brings this energy technology to the fore. Since current wind turbines are widely used in power electronic systems, the research focuses on complex technologies such as electronic converters and advanced control systems. The review of literature has been made with articles on possible problems and control methods that may occur in the grid connection

of DFIG wind turbines. The area of the studies is to use innovative methodologies, models, and simulations to solve power system transitory difficulties that develop when a direct grid connection exists at a wind farm.

In this thesis, it is aimed to model a 2.6 MW wind turbine with a doubly fed asynchronous generator mathematically by vector control method. In the further parts of the thesis, the vector control method will be simulated with the Matlab/Simulink program and a voltage problem between 3-3.1 s will be created and the effect of the crowbar circuit on the recovery of the system will be examined.

The thesis aims to design a simulation with real turbine parameters for a wind turbine with a doubly fed asynchronous generator. With this simulation, the stability of the system in integration with the grid is examined and the response of the system in case of a temporary fault and at various wind speeds is analysed. The discontinuous wind characteristics affect the system stability of the grid. Fast and real-time simulations are performed utilizing MATLAB/Simulink software to examine the significance of the chosen DFIG on the electricity grid. The designed simulation assesses the performance of wind power plants and system protection status using a model. A simulation model is designed to examine the behaviour of the system in the event of a grid fault. A DFIG model is developed to simulate voltage dip, and the simulation outputs which illustrate the behaviour in the event of grid fault are examined.

This thesis aims to investigate the impact of utilizing DFIGs on the behavior of power systems during grid faults. Existing literature indicates that there are differences between simulation results and experimental data, primarily due to reactive power considerations. In simulations, the reactive power is controlled through the converter's control system. In the literature, the ideal converter is used, assuming a constant voltage on the DC bus between the converters.

Based on the information gathered from articles, various assumptions, analyses, and simulations are conducted to address the challenges associated with integrating DFIG-based wind turbines into the electricity grid. Case studies utilizing existing turbine data, along with new approaches and methods, are developed to enhance the performance of DFIG systems. The objective is to minimize issues and ensure reliable grid connection. The findings of these studies, which combine theoretical analysis and simulation results, are presented in the literature. The thesis aims to investigate the ability of the system to continue contributing to the grid in the event of a symmetric fault for a DFIG-based wind

turbine. For this purpose, the voltage drops created in the stator voltage were analysed using the Monte Carlo method with 1000 possible Vs and Ir values and the amount of increase in the rotor current caused by the percentage decrease in the stator voltage. Thus, the ability of the system to continue contributing to the grid was investigated by predicting the effect on the rotor current before a possible symmetrical fault.

CHAPTER 2

LITERATURE SURVEY

In this part of the thesis, the wind turbine classes present in the literature will be investigated. The types of generators commonly used in wind turbines are explained in detail, and then the converters used in the sector are briefly summarized. Then, wind turbine control systems will be examined, the requirements related to the grid will be explained, and faults that occur in the grid will be detailed.

2.1. Wind Turbine Classification

Wind turbines are machines that convert the kinetic energy from the wind into mechanical energy and then into electrical energy through a generator. It has mechanical and electrical components in its structure. Considering the thesis content, types of wind turbines are classified under 2 main topics: Wind speed and Power train.

2.1.1. Wind Speed

Wind turbines are categorized into two groups based on wind speed: Fixed Speed Wind Turbines (FSWT) and Variable Speed Wind Turbines (VSWT). FSWTs are robust and reliable besides having a simple mechanism. However, reactive power is uncontrollable and increases mechanical stress in FSWT.

On the other hand, VSWT is to provide maximum aerodynamic efficiency at variable wind speeds. A power converter connects VSWTs to the electrical grid. The energy capture is high in VSWT, it improves power quality and reduces mechanical stress. VSWTs present today have been developed to maximize system stability. Besides, wind

turbine configurations are classified according to power control and speed control. Four different wind turbine concepts have been developed for speed control. Turbines are divided into various concepts under the titles A, B, C, and D concepts according to their speeds. The A concept (fixed speed) is created for a rotor that rotates a grid-connected converter at a fix-speed for an asynchronous Squirrel Cage Induction Generator (SCIG). Since SCIG's reactive power is frequently obtained through a grid, this design employs a reactive power compensation bank. Wind fluctuations cause mechanical changes in a wind turbine and hence electrical power fluctuations, regardless of power management theory. In the case of a grid fault, the voltage at the junction can be distorted. Because of all these voltage variations, reactive power is generated by the wind farm using the magnet, and voltage instabilities and losses in transmission occur. The A concept principal's disadvantage is that it does not permit rate modulation, needs a grid, and increases mechanical stress (Ackermann and Thomas, 2012). Figure 1 depicts the system diagram of concept A.

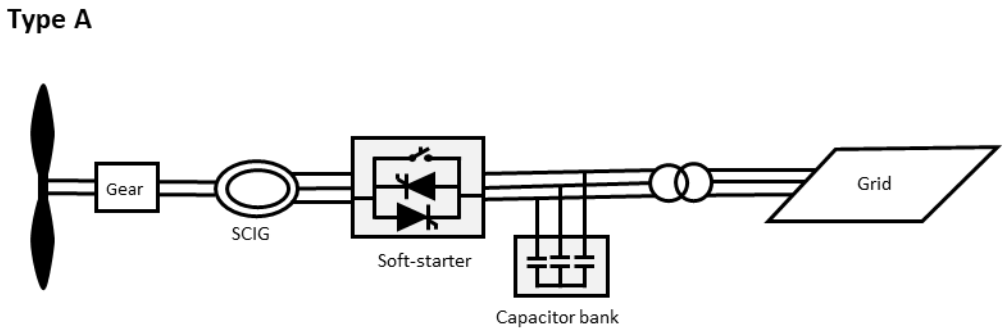

Figure 1. Concept A system

Variable rotor resistance generator is used in wind turbines, namely the B concept (with only a small range of speed). The motor is directly connected to the power grid, and the reactive capacity is balanced by a capacitor bank. A soft start increases grid connectivity. This design is distinctive because it incorporates a variable added resistance of the rotor that is adjusted using the rotor shaft and an optical converter that allows monitoring of the overall rotor resistance. Variable rotor resistance depends on the dynamic speed regulation spectrum (Ackermann and Thomas, 2012). The system diagram for the B concept is illustrated in Figure 2.

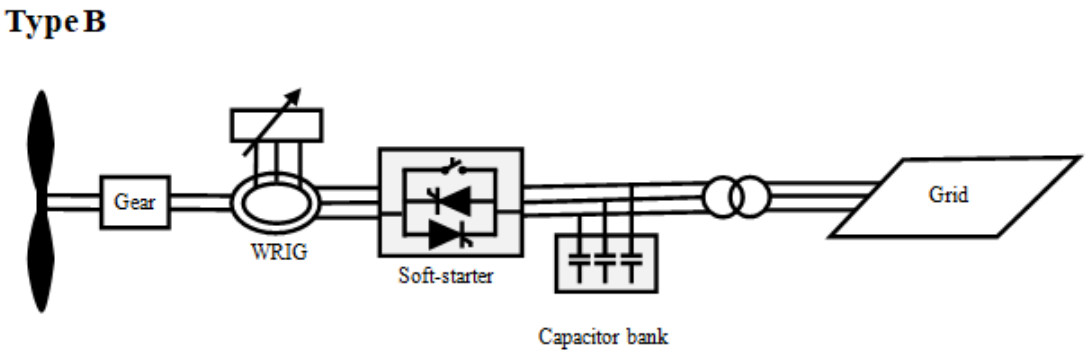

Figure 2. Concept B system

In the thesis, the design of a type C wind turbine (variable speed with partial scale frequency converter) has been taken into consideration. This idea, which is also known as the DFIG idea, is a partial-scale frequency converter with variable speed. Today, the most prevalent wind turbine generator types the doubly fed induction machine is used in capacities larger than 1 MW (Saini and Shilpi, 2013). The fact that a partial amount of the generator's power is transmitted to the power converter is one advantage of the DFIG design. Usually, this only corresponds to 20–30% of the capacity and has a significant cost advantage for the asynchronous generator-based turbine concept compared to a full-scale converter model. The system diagram for the C concept is explained comprehensively in the operating principle of the DFIG.

In the D concept wind turbine (the variable speed with full-scale frequency converter), a frequency converter with the generator is connected to the power grid at full capacity. Reactive power is balanced by the frequency converter and contributes to the supply of the grid wound-rotor synchronous generator (WRSG). In order to excite the generator, a rotor induction wound generator (WRIG), or a permanent magnet synchronous generator (PMSG) might be utilized. Some types of wind turbines, that do not have a fully variable speed gearbox, utilize a large-diameter multipolar direct-drive generator (Ackermann and Thomas, 2012). The system diagram for the D concept is illustrated in Figure 3.

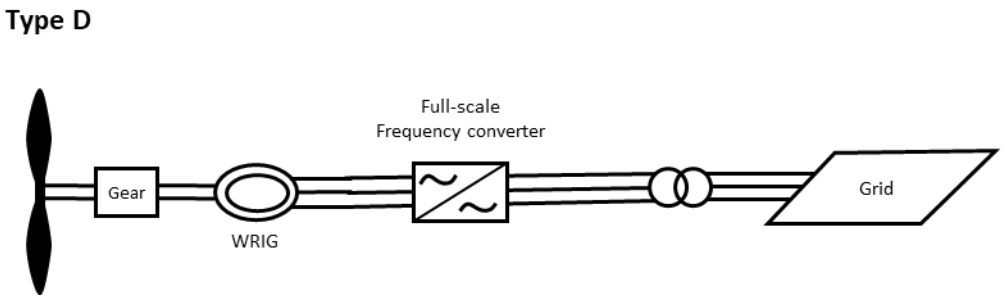

Figure 3. Concept D system

2.1.2. Power Train

In modern wind turbine technology, there are two types of generator drive methods: direct drive technology and gearbox (Gagnon and Richard, 2005). Direct drive technology is used in synchronous generators. In this method, the wind turbine blade rotating at a low speed directly drives the synchronous generator. The disadvantage of this method is related to the power electronic circuits, which are used to transfer the power produced by the generator to the grid. The stator of the synchronous generator is connected to the grid via a power electronics circuit. Therefore, the total power of the generator is directly transferred to the grid via the power electronics circuits. This situation complicates the design of power electronic circuits especially at high power and increases the cost. Conversely, the gearbox is used in wind turbines with asynchronous generators. In these systems, the gearbox drives the low-speed turbine blade and the asynchronous generator. In these applications, DFIG is commonly preferred. The stator of the DFIG is connected to the grid directly. Power electronics circuits regulate the generated power via the rotor windings. The main advantage of this technology is that the power flow through the rotor of the DFIG is around 30% of the total power of the generator, thus the design of the power electronics circuits is simpler, and the dimensions and cost are decreased. The main problem with this system is that the system gearbox frequently causes breakdowns.

2.2. Generators Used in Wind Turbines

Wind turbine generators convert mechanical energy into electricity. In general, 3 types of generators are used in wind turbines. These are direct current, synchronous, and asynchronous generators.

2.2.1. Direct Current Generators

Since the speed controls of direct current generators are practical, they are used in wind turbines. The alternating current produced is converted into direct current with semiconductor rectifiers. Due to the limited capacity and power of permanent magnets, they are preferred in low-power wind turbines and off-grid systems (Patel and Mukund R, 2021).

2.2.2. Synchronous Generators

Synchronous generators compared to asynchronous generators are at a high price and mechanically more complex. Synchronous generators are more suitable for fix-speed systems and operate at fixed frequencies. The direct current in the rotor used in wind turbines is supplied from the grid. AC is taken from the grid and converted to DC and transmitted to the windings of the rotor via brushes.

2.2.3. Asynchronous Generators

The asynchronous generators generate maximum performance in the changes in wind speed, that is in power changes. When the wind speed exceeds the nominal value, it protects the mechanical parts by reducing the vibrations that occur in a moment. Since

the speed of the rotor blades is adjusted by the gearbox, it can be easily connected to the grid without being synchronized with the grid.

2.3. Converter Used in Wind Turbines

With the development of wind turbine technology and the reduction of costs in power electronics, different types of converters are developing for turbines. Converters used in wind turbines are matrix converters, tandem converters, frequency converters and back-to-back converters.

2.3.1. Matrix Converters

Matrix converters are known as AC/AA converters in the literature (Coşkun, İsmail, Ali Saygın and Mahir Dursun, 2008). This type of con6verter is to obtain voltage at the desired frequency from the source by connecting the ends with switches. Since there is no capacitor in the DC bus, its input and output are combined. This affects the output power in case of unbalanced load and voltage (Hansen and Lank Henrik, 2001). Fault protection for matrix converters is not as successful as cascade converters (Melicio, Mendes and Paulo, 2010).

2.3.2. Tandem Converters

Tandem converters used in wind turbines operate an active filter to compensate for harmonic distortions occurring in the bidirectional frequency converter (Hansen and Lank Henrik, 2001). Since it is a current source converter, there is no voltage increase between the input and output terminals because of the capacitor connected to the DA link in the secondary converter, but applying a current source converter as the primary

converter only reduces the usability of the grid voltage. This means more current flows through the generator.

2.3.3. Multi-Level Converters

The purpose of using multi-level converters is to create sinusoidal voltage by using capacitors at various levels of voltage sources. They are converters that necessitate fewer filters and can provide high voltage (Hansen and Lank Henrik, 2001). The total switching frequency can be reduced to 25% of the two-level converter.

2.3.4. Back-to-Back Converters

A bidirectional frequency converter consists of two voltage-fed converters. It has a DC bus and capacitor in its structure. The DC bus voltage should be kept higher than the voltage of the grid to control the grid current. To obtain the desired voltage, capacitors can be connected in series or parallel according to the application. The output voltage level is generally 380V – 690V (Islam, Rabiul, Guo and Zhu, 2013). As a result of this, a step-up transformer is used to increase the voltage at the converter output. Since there is a capacitor between the generator and the grid, it allows independent operation and control of both. Since it is the generator used in the thesis study, it will be explained in detail in Chapter 5.

2.4. Wind Turbine Control Systems

For stable operation and optimization of the turbine, a wind control system is required. System control is extensive due to a lack of continuous, consistent wind in wind turbines and its heuristic nature. With the system control of wind turbines, it is simple to exert control of the wind when it reaches the nominal wind speed. The turbine is cut in

and cuts out within a certain wind speed range. In the partial load area, energy from the wind is maximized. Turbine parts are isolated from multiple fatigue loads.

2.4.1. Configuration of a Variable-Speed DFIG Wind Turbine System Control

In the event of a grid fault, DFIG wind turbines must continue to supply power to the grid. The control capability of wind turbines based on a case of grid fault involves both wind turbine control to avoid over-speed as well as power converter control and safety during and after grid faults.

There are various types of control methods in wind turbines:

- Aerodynamic control
- Drive train
- DFIG control

2.4.2. Aerodynamic Power Control

The aerodynamic wind turbine's power control is applied to prevent the turbine from capturing full power in the partial load area below-rated wind speed and being affected at speeds above the rated speed and also applied to make certain that the power remains constant at the optimum turbine speed level (Takaai and Hitoshi, 2010). The ideal power curve of a typical wind turbine is shown in Figure 4. Due to the low wind speed in Zone I, the turbine is closed and does not produce electricity. The second field is the partial loading area. Here, with assistance from the control system, the wind is attempting to maximise energy extraction. The third zone is the entire load area in which the wind reaches the nominal speed. The rotor's speed, and hence the generator's power, is maintained in this area with various control techniques. The turbine is deactivated to ensure that the device does not damage when the wind speed exceeds a nominal speed.

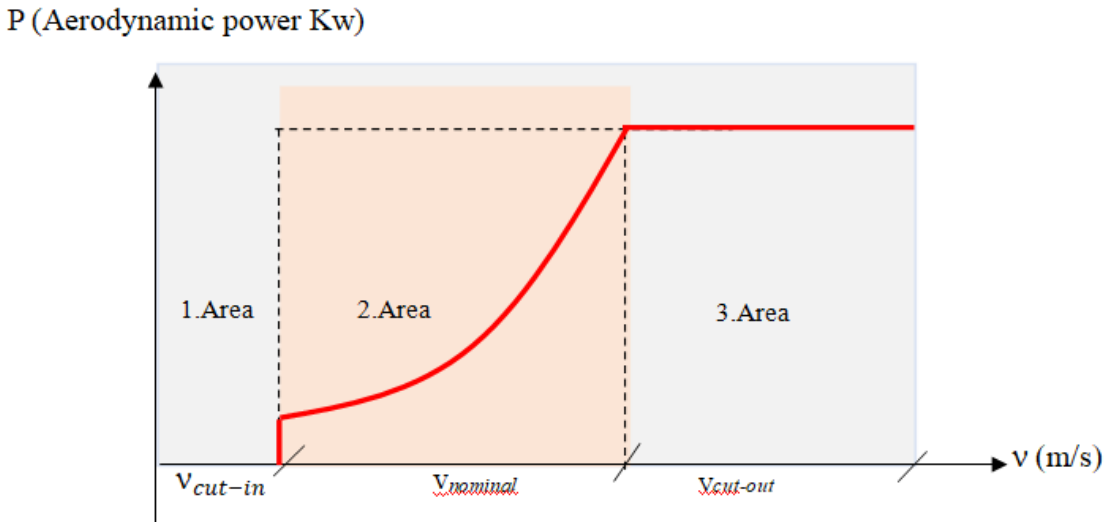

Figure 4. Optimum power curve about a wind turbine

The techniques utilized to take the turbine power curve under control and closer to the ideal value are as follow.

- **Passive Stall Control**

Stall control is based on the idea that less wind energy should be used because of the turbulence effect on the blade due to the angle of the airflow blades (Burton and Tony, 2011).

- **Active Stall Control**

With active blade angle control in wind turbines, whenever the wind speed exceeds the nominal value, to minimize the attack angle, the blades are turned. In the active stall control, the blades are rotated in the inverse direction to stop the turbine and power control (Burton and Tony, 2011).

- **Passive Pitch Control**

While designing with passive angle control, by twisting the blade to achieve the proper blade angle, the power at high speeds is limited and provides power control (Burton and Tony, 2011).

- **Active Pitch Control**

By employing active blade angle control, the angle of attack is adjusted through larger blade rotations to maintain a consistent turbine output, considering the nominal wind speed. With this system, the energy capture rate is increased, and the wind load is reduced when the turbine is deactivated, braking becomes easier (Burton and Tony, 2011).

- **Yaw Control**

The yaw control mechanism is implemented to prevent the Wind Turbine (WT) from exceeding its rated capacity in terms of speed and power. The objective is to optimize power generation by allowing the WT to operate below the wind speed at the maximum power point while maintaining a zero-yaw error. This is achieved through the utilization of two PI controllers operating in different regions, collectively forming a yaw controller. By effectively nullifying the yaw error prior to the WT surpassing its rating capacity, the yaw controller aligns the WT with the wind direction, thereby ensuring the overall stability and protection of the WT mechanism (Shariatpanah,Hamid, Fadaeinedjad and Rashidinejad, 2013).

2.4.3. Drive Train

A wind turbine's drive train includes a gearbox and generator, which are required for a turbine to generate power. The gearbox connects the low-speed shaft to the turbine blades and the high-speed shaft to the generator. The gearbox controls the sluggish spinning of the outer blades.

2.5. DFIG Operating Control Mechanisms

In the use of an asynchronous generator (DFIG), whose rotor is connected to the Voltage Source Converter (VSC) by slip rings, the VSC is connected to a control system that determines the voltage it applies to the rotor of the induction generator. This provides a variable speed feature that optimizes power generation. By controlling the rotor voltage, the VSC controls the current drawn from the grid. The voltage VSC exerts on the rotor is determined by the speed, torque and voltage. These are the controllers included with the VSC. In DFIG, the voltage source converter consists of two parts with a DC link between

them. The voltage source converter connects the rotor to the grid. DFIG components are listed as follows:

- Wind turbine
- Gearbox
- Induction generator
- Converters (VSC)
- DC link
- Voltage controller
- Speed controller
- Torque control

The purpose of VSC is to provide the rotor voltage. The VSC control determines the rotor voltage and uses speed, torque, and voltage controllers for this purpose.

DFIGs are gaining popularity in wind power generation, and comprehending their control systems is of utmost importance. In DFIG, the converter feds the rotor. Rotating reference frames that are synchronized with the flux of currents in the stator and rotor are regulated. In on-grid systems, the rotor and stator are both connected to the grid. The machine's electrical torque is mostly controlled by Maximum Power Point Tracker (MPPT).

The vector control frame is produced using the oriented frame. For the stator voltage vectors, instead of rotor flux stator current is used. The dynamic output analysis of these controlled currents is similar, nonetheless, the stator current components are inversely proportional to the stator's capacity for active and reactive power along the d and q axes. Rotor Side Converter (RSC) stands for uses the Pulse width Modulation (PWM) technique. Besides, the PWM models are shifted to reduce the maximum applicable harmonic distortion. The DFIG control method is more complicated than the conventional induction machine control method. For DFIG control, an electronic converter for power controls the rotor current for regulating the rotor. The 3-phase matrix conversion system of DFIG control is an alternative to the PWM method as a voltage-induced converter. For DFIG current, a vector (field-oriented) control system is used.

2.5.1. Generator Power Control

Active power control (torque control) is done separately from reactive power control. Reference values are considered for both controls. The blade is adjusted to operate at lower wind speeds to maximize power extraction from the wind. The power attained from the wind is lower than the nominal power of the generator. To confirm the turbine operates within acceptable limits at high wind speeds, the blade angle is controlled to limit the power absorbed by the rotor to the nominal power of the generator (excluding losses). It is critical to generate electrical power that strictly matches the mechanical power of the turbine rotor, preferably without any significant losses. In this context, the mechanical power of the turbine rotor assists as the reference power for the generator (Shi and Libao, 2009).

2.6. Conversion System of Wind Energy Grid Connection Problems

The fact that wind turbines are affected by changes in wind speed has different effects and functions on grid efficiency than conventional power plants. There are studies in the literature on the problems that occur in the electrical grid to which the wind turbines are connected. The effect of wind turbines on the structural integrity and operating characteristics of the electrical system and the technical specifications for the connection of the wind farm to the grid are examined. Various methods and models have been used to describe the problems. DFIG generators are often used for Wind Energy Conversion Systems (WECS). Typically, these generators are connected to the grid via electronic power converters to regulate frequency, voltage, and power flow as wind speed changes.

2.7. Grid-Connected Wind Farms Effect on Power Quality

IEC 61400-21 standard for wind turbine power efficiency: IEC is defined as" distribution and assessment of the characteristic wind farm with grid connection power

efficiency” by the International Electrotechnical Commission (IEC). This standard specifies the requirements typical of wind turbine operation regarding power performance and also proposes measures and characteristics of the power quality of wind turbines connected to grids. Although the standard defines mainly assessment methods for the designation of single wind turbines, it also includes techniques and models that allow single turbine system parameters to be extrapolated to the typical product quality of wind farms under pre-defined conditions. No standard protocols were in force before IEC 61400-21 was established. Since variance in voltage and flickering are influenced by differences in grid power flows, wind farms' operations can affect the grid voltage. At the local level, the main concern with wind power is voltage fluctuations.

When the IEC 61400-21 standard was published for the power quality of wind turbines, the main subject of study was essentially the voltage performance of the turbines. The reason for this is that wind turbines were primarily connected to the electricity grid at the time the specification was created. The main issue is the potential impact on the voltage output rather than the performance of the power system. The development of huge wind turbines, which can form an important part of the energy transfer to the grid, has been improved by these standards and tests.

2.8. Grid Code

The most important issue is the system's stability for the electricity system. System stability is examined under two headings: frequency and voltage stability. Long and short interruptions are important for frequency and voltage stability. In this thesis, voltage dips occurring in the power system are emphasized. Faults occurring in the grid are defined as single, two-phase asymmetric, and three-phase symmetric. Within a hundred milliseconds from the moment the error occurs, the protection units (crowbar) are removed from the fault part of the grid, and the power system recovers stability in a few seconds and continues to operate. When a positive sequence error occurs, the frequency of the generator and motor perhaps unbalanced according to power system theory due to the low voltage of the grid. Since the low grid voltage will cause serious

problems in the electrical system, the stability of the system should be ensured by increasing the low voltage according to the nominal value during the frequency of faults, and voltage-induced faults are important for both active and reactive power. When grid electricity is recovered, active power consumption in the power system components is recovered. To solve these problems, power plants must remain connected to the electrical grid and return to stability when a problem occurs. This will be possible with the help of protection units.

With increasing renewable energy generation worldwide, the contribution to the grid is expanding. Countries using wind energy are conducting studies on grid codes for wind energy integration. In grid codes, a wind power plant's primary frequency regulation, voltage control, synthetic inertia, and oscillation damping functions should respond to the damping functions for oscillations and contribute to the electricity system's frequency and voltage stability. The situation where the wind turbines continue to contribute to the grid during a fault is defined as Fault Ride Through (FRT). The wind farms need to inject reactive current and grid voltages to reach the nominal value of the grid voltage. The importance of a grid fault is usually related to the voltage drop during the fault and the duration of the fault. The voltage drop caused by the fault is analysed using the fault impedance in addition to the grid power. Grid codes for wind farms and turbines are studied to understand the response to faults. Covers wind power plants based on voltage levels for transmission and sub-transmission with VDN in the German grid code, this is one of the most popular major grid codes. The purpose of the codes is to reveal the FRT needs for the WECS. Even if the voltage drop is zero for the FRT, WECS require being dependent on the grid.

2.8.1. Grid Code Requirements

There are rules that the power plants must comply with in terms of electricity quality and reliability for the grid connection of wind farms. These rules are known as grid codes and are arranged for transmission, distribution, and users of the system.

Four key factors affect power quality:

- Harmonic distortion
- Flicker
- Sudden Voltage Step Changes
- Voltage Imbalance

The status of the electrical grid-connected system is evaluated to determine the level of power and ensure stability for high voltage. IEC 61400-21 is an International Standard for determining wind turbine construction within the most appropriate parameters and measurements. When determining power quality for wind turbines, it is important to define the electrical properties. National standards developed in different countries contain the necessary conditions for determining power quality. Additional considerations regarding wind turbine and wind farm grid integration, as well as grid backing in case of grid faults (voltage drops) and reactive and active power control, are available in country grid code documents.

2.8.2. Fault Ride Through

Voltage dips may occur when WECSs are connected to the system under different fault scenarios and negative effects such as instability and inefficiency occur in the connection of WECs. To solve these problems, grid codes have been developed and WECSs are intended to contribute to the grid even in unfavourable connection situations. These contributions, known as FRT capability, are defined as operating and restoring active power after faults by injecting a reactive current that supports the voltage even if the voltage drop reaches very severe levels.

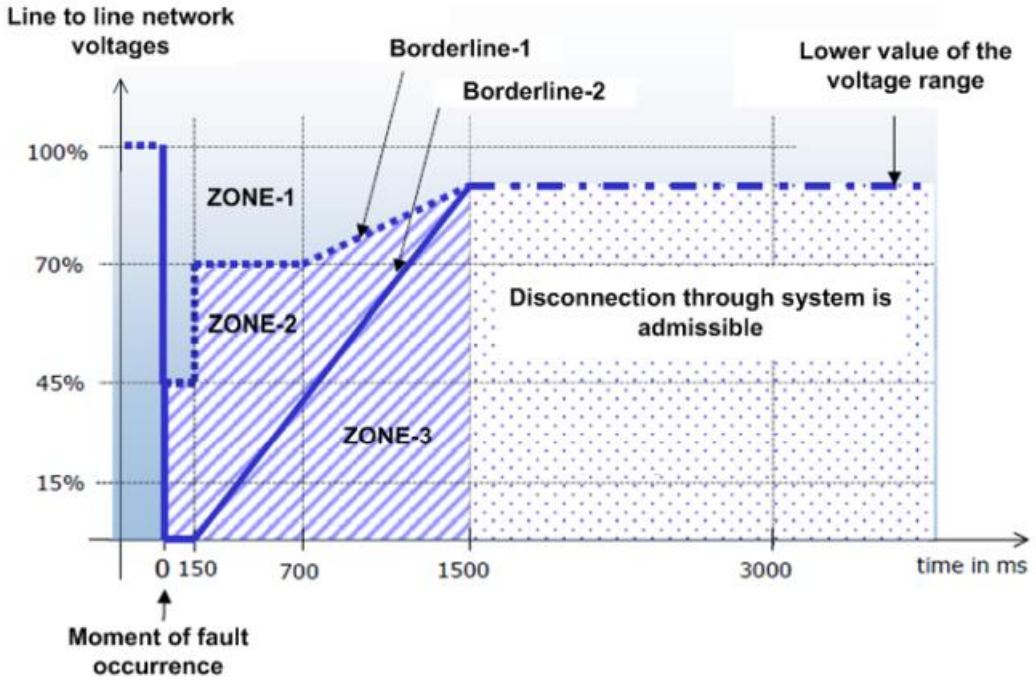

Figure 5. Wind farm FRT requirement

The curve shown in Figure 5 defines the FRT is defined as the voltage curve that is connected to the grid. Shaded areas are described as follows.

1) The symmetrical voltage drops, and short circuits given in Zone 1 should not cause any instability in the electrical system of the wind turbines due to disturbances and should ensure that the connection is not disconnected.

2) There are two options in Zone 2. The first is that during the fault wind turbines must be connected to the system grid. If the wind turbines cannot supply the requirement, the limit can be changed by agreement with ISO. Another option is to temporarily disconnect the wind turbines from the system, provided an agreement has been established with the TSO, in case the turbines0 are destabilized, or the generator protection is activated (Netz,2006).

3) Short-term disruption from grid wind turbines is considered in zone 3. It is also allowed to disconnect wind turbines through protection systems.

2.9. Problem Formulation of The Grid in Wind Energy

Some transient faults may occur when the wind turbines are connected to the grid. These problems are common in the reviewed articles. Before the turbine is connected to the grid, performance problems are identified, sensitive control codes are allowed to be used and a high degree of security is provided. Some regulations require wind turbines to remain connected to the grid during temporary faults (Pannell, Graham, Atkinson and Zahawi,2010). To keep the voltage and frequency of the grid constant after a transient fault, the generators should continue to provide active and reactive power to the grid. In other words, the wind turbine should contribute to the grid. These variables are related to the FRT capability. Grid transient faults in wind turbines are examined under several topics. One of them is the short circuit problem. For the solution, analysis is made with crowbar circuits and approaches to short circuit currents are developed with these analyses (Morren, Johan and De Haan, 2007). When there are voltage fluctuations in the grid, the flickering that occurs in the continuous wind turbine's operation is another problem and this problem has been examined in the literature (Sun, Tao, Chen and Blaabjerg, 2005). A sudden voltage drop is another serious problem for a grid connected DFIG. These sudden drops can cause the converter to malfunction (Lopez and Jesus, 2007). All these problems will be explained in detail in the next section. In the following parts of the thesis, the response of the system in case of a sudden voltage drop will be observed by simulation.

2.9.1. Severe Fault Considerations

Transient faults that may occur in the wind turbine grid connection are detailed below.

2.9.1.1. Short Circuit

Crowbar circuits are preferred to control overcurrent's that will adversely affect RSC during voltage drops in the system (Lei and Yazhou, 2006). The main purpose is to maintain the converter's connection to the generator by allowing power injection into the grid during a fault. Thus, grid disconnection is prevented, and the controllability of the system is increased. The development of RSC-specific control algorithms that can reduce overcurrent's in the windings of the generator without opening the converter in case of fault is important in modelling. With the developed control methods, it is concluded that the overcurrent's can be controlled in a few milliseconds. How the setpoint can be applied for one learns about the rotor current controller from during the moment of fault, measured stator current values. With the developed control methods and simulations, it is recognized that testing the reliability of a DFIG under severe electric grid challenges is possible without the need for extra supplementary circuits. Wind turbine conversion systems are highly susceptible due to a faulty power switch. A power switch that fails unexpectedly lowers system performance and may result in disconnection. Therefore, the fault must be identified and resolved quickly, or it may cause permanent faults. Various techniques have been examined to identify the fault, voltage power converter with three phases is used (Karimi and Shahram, 2008). Using these techniques, it was possible to fix the fault within a quarter of the primary cycle.

2.9.1.2. Flicker

When connecting the wind turbine to the electrical grid, it can generate vibrations. This can be a limiting factor if we want to integrate turbines into grids with high wind power penetration. This situation occurs when there are voltage fluctuations in the grid. Variable wind speed can occur due to wind pitch and tower shadow effect. With the analysis, the most effective way to reduce vibration must regulate a wind turbine's reactive power production while ignoring average wind speed, and the short circuit capacity to turbulence intensity ratio. In simulations, to effectively simulate, a small

simulation time step is necessary to analyse PWM waveforms. This causes the simulation speed to slow down, so the proposed model for a voltage source converter with PWM in detail is not suitable for flickering calculations that need a simulation duration. To simulate a large time step, a keyless averaging model should be preferred because the operation does not concentrate on the keys of the PWM converter, thus increasing the simulation speed. When wind turbines reach their rated power, the level of vibration for higher wind speeds is reduced. The DFIG can correct for fluctuations caused by turbulence reflected from the wind's output power in a variable speed combination operation and pitch angle modulation. It has been determined that the flickering is caused by voltage fluctuations, and reactive power is rearranged when the real power is changed. Controlling the turbine's reactive energy output is also important for vibration reduction, and these are shown in the simulations (Peterson and Andreas,2005).

2.9.1.3. Voltage Drop

One of the main problems for grid-connected wind turbines is voltage drops (Bongiorno, Massimo and Thiringer, 2013). A sudden drop causes a drop in grid voltage overcurrent’s in the rotor's windings and can if no protective component is provided to the system, the converter may malfunction. As wind energy becomes more common, voltage drops in wind turbines have become a significant subject of study. The behaviour of the generator during voltage drop is carefully examined and the source of the problem is studied. To solve this problem, when the turbines are associated with the grid they must contribute to the grid's stability and dependability. For this, the system must support the grid when it encounters a fault. With the revised grid codes for modern turbines, turbines can provide grid electricity, both active and reactive now. Because when a fault occurs, DFIG can lose some of their magnetization feature or vector control, and even lose active and reactive power. For these reasons, FRT modelling is being developed. FRT standards have been established in the industry (Wessels, Christian, Gebhardt and Fuchs, 2010). These standards require that the wind turbine remains in system faults and ensure the voltage drop in the turbine connection when a problem occurs. For each turbine, specific voltage profiles are given by grid operators to verify its ability to withstand voltage drops.

Existing wind turbines meet FRT requirements regardless of the specific turbine type. DFIG based wind turbines must be connected to the grid during grid faults to maintain the grid's stability, based on grid principles. This condition complicates generator and converter management and protection. If there is a power outage, DFIG control capabilities include control and protection of wind turbines. Such as overspeed, and power converter control and protection during and after grid faults. In one of the studies, a Dynamic Voltage Restorer (DVR) was applied as a solution to sudden voltage drops. The DVR can solve the issue. DFIG wind turbine can continue to operate with fault line voltage running nominally as expected from real grid codes. When the system of the DVR protects the wind turbine, the voltage drop issue perhaps resolved. These solutions have been demonstrated by simulations (Bongiorno, Massimo and Thiringer, 2013). While using the RSC, the stator may separately manage both reactive and active power and in grid coding, reactive energy is produced by maintaining the speed constant during the planned grid faults. With the analysis and simulations, it was concluded that the use of DVR is an appropriate approach for protecting the DFIG system from asymmetric grid voltage errors (Lopez and Jesus, 2007).

2.9.1.4. Aerodynamic Problems

In studies, mathematical equations related to wind turbine aerodynamics are derived (Yazdani, Amirnaser and Iravani, 2010). Pitch control wind turbines have been developed to prevent damage to the turbine by keeping the high speed at nominal power when the wind comes to the turbine at a higher speed than the rated speed. It is important to follow the torque-speed curve. The presented method uses the active power setpoint using the current to manage the stator fluctuation frame of reference for the rotor speed and current, to receive the necessary active power outcomes and optimal torque in generating the desired speed and torque. Fluctuations in wind speed push the turbines to operate outside the maximum of the Cp curve. This situation causes high mechanical stress and is transmitted to the electrical system. This situation is unfavourable in terms of capturing energy. To resolve these problems and assure the system's smooth functioning, the link between turbine wind speed, the maximum allowable rotor speed

and the nominal power has been studied (Beltran, Brice, Benbouzid and Ahmed-Ali, 2012).

The generated electromagnetic force in the machine rotor is one of the primary issues for DFIG. This problem has been solved by knowing the current and voltage capacity on the rotor side of the converter by using control method approaches to increase the solution probability in case of grid faults (Xiang and Dawei,2006). For DFIG, control to pass through the grid faults is difficult and this is a negative situation for the market. Approaches such as when the main power supply fails, increasing the voltage at the generator's connections and optimizing the current control loop parameters within the rotor-side converter have been developed. Control algorithms have been derived, making it easier for the system to pass through the grid fault that considers the machine's internal state. The application of robust control mechanisms like quadratic shifting mode allows direct control of DFIG torque to eliminate some errors (e.g., non-optimal power extractions). With this control, no extra mechanical stress occurs and provides durability for limited access time, generator, turbine, and external disturbances (grid). Aerodynamic controls are complex systems when it comes to large-scale turbines. The primary goal of the management of wind turbine speed variation is to increase the extraction of power. Regardless of the fluctuating speed of the wind, it is essential to regulate the generator's production of electricity by maintaining an optimal turbine tip speed ratio. When an induction generator exceeds synchronous speed, it transmits actual electricity to the grid and simultaneously draws to fulfil the magnetization and reactive power requirements, grid-supplied inductive reactive power. With the simulations made, it was concluded that the injected rotor voltage affected the DFIG. By altering the phase angle and amplitude of the injected voltage, the rotor's speed is reduced from over to sub-synchronous to produce power. Moreover, it increased the thrust torque of the DFIG. It has been observed that DFIG is capacitive when operating with asynchronous speed generation mode and otherwise inductive (Byeon, Gil-Sung,Park and Jang, 2010).

CHAPTER 3

METHODOLOGY

In the first part of this chapter, the working principle of the doubly fed asynchronous generator and the back-to-back converter is explained. Then, the methodology of the field-oriented vector control method for the converter control system is presented.

3.1. Operating Principle of the DFIG

Doubly fed induction machines are generally used for a relatively limited speed range and in applications requiring high electrical power. Different speeds will provide various advantages: the speed of the rotor can vary by wind speed, thereby enhancing wind turbine efficiency, reducing mechanical stress, and not transmitting the vibration of torques into the grid. Considering all types of turbines, DFIG's use in industry is increasing day by day due to its advantages. Modelling for DFIG is done with various assumptions and simulations. The simulations are performed to understand the fit between models and theory and to use and develop them in the site. Simulations evaluate the performance of equipment by examining the system protection, workspace, and on-site tests, as well as checking the performance of power plants. In addition, the simulation results give information about the method to be followed to overcome the fault and the recovery time.

Wind turbine system control based on DFIG requires understanding the mathematical model RSC and GSC first. Generalized dynamical equations of electrical machines are used while modelling. These equations are examined under two headings, mechanical and electrical. While the generator model is used for the rotor side, electrical

equations are used for the grid side. Based on the machine dynamic equations in 3 phases, first, the mathematical equations for the generator were given, then the axis transformation was applied to the obtained equations and the dynamic equations for the generator were examined in another axis set.

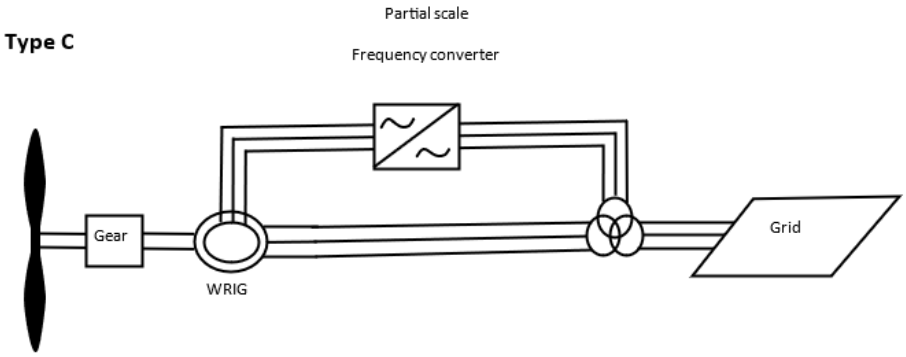

Figure 6. Concept C system (DFIG)

In DFIG, the stator is directly connected to the grid; The wound induction generator has slip rings with back-to-back interface through a partial-scale power converter. DFIG is fed twice; the first one is realized by the application of a voltage produced by the grid on the stator and the second one by the power converter induced by generating voltage at the rotor. As shown in Figure 6, the converter has a common dc bus connecting the RSC and the GSC. The magnetic flux in the DFIG is generated by the rotor and the stator windings are fed from the grid. Modulating (PWM) converters control stator and rotor currents. When the rotor of the DFIG starts to rotate faster than the synchronous speed, the machine starts to generate electricity.

The voltage frequency induced in the stator must be the same as the grid frequency. By replacing the frequency supply of the rotor with PWM converters, the stator frequency can be kept constant. PWM converts the fluctuating magnitude and frequency voltage at the rotor terminals of an induction generator into direct current voltage. This technique is independent from speed, which is one of the primary reasons why DFIG is preferred in variable-speed applications. Typically, a pair of converters connect the stator windings and rotor windings of the DFIG. The output voltage is adjusted by converters to keep the system running smoothly at a wide range of speeds as it generates both reactive and active power. The rotor of wind turbine is connected to the electrical grid

using a back-to-back converter in a partial-scale power converter that is based on the DFIG idea and has variable speed. In wind turbine power plants, when the grid voltage dip or three-phase short circuits occur, there are increases in the DC-link voltage level, rotor current, and rotor speed between the converters. These increases are mitigated within predetermined limits before they reach significant levels by grounding the faults through crowbar and chopper circuits. The chopper circuit is typically used to mitigate faults caused by low-level rises in the DC-link voltage, while the crowbar circuit comes into operation when the chopper circuit proves insufficient, ensuring the fault is grounded. A crowbar is attached to the converter to protect the converter on the rotor side. At a broad range of speeds, from super-sync to sub-sync speeds, DFIG will provide energy for the grid. Normally, in synchronous speed, DFIG's variable speed range is ± 30 percent. This means that only 30% of wind turbine output is converted to the back-to-back converter's rated power. It operates the converter's rotor side active power and is optimized with the aid of the generator speed to achieve wind power.

3.1.1. Power Converter

In the literature, the average AC / DC / AC converter model is utilized for a DFIG (Gagnon and Richard, 2005). Common elements of power converters include grid side control, power control, rotor side current control, and dc-link dynamics. The RSC and GSC are the converter's AC/DC/AC components. It is known in the literature as a voltage-based converter. A capacitor that is DC-coupled and utilizes force-modified power electrical components. Insulated Gate Bipolar Transistors (IGBTs) function as a DC voltage source created by converting a direct current voltage to an alternating current voltage. While the three-phase stator winding directly connects the power grid, the three-phase rotor winding is connected to the RSC through slip rings. After being transformed into electrical energy, the collected electricity windings on the stator and rotor allow energy from the wind turbine to be sent to the grid. With the control system, the voltage at the grid terminals regulates the power of the wind turbine and the voltage on the DC bus. RSC and GSC generate the voltage and pitch angle command signals Vr and Vg, respectively. IGBT is used to obtain alternative current voltage from a direct current

voltage source as the converter components. As explained in the studies examined, the rotor and grid can create or absorb reactive power and can be utilized to manage reactive power or voltage at grid terminals (Babu B.,Chitti and Mohanty, 2010). The control of the RSC rotor current controller aims to stabilize the power/torque value at a lower point.

3.1.2. Pulse Width Modulation (PWM)

PWM is a method for producing the required analogue electrical value or signals at the output by managing the widths of the pulses that will be generated. PWM inverters use to regulate the rotor current in the DFIG-based wind turbine, thus separating the active and reactive power on the stator side. The best-known PWM is sinusoidal. The triangle (carrier) wave at the point determined by this method is compared with the sinusoidal wave. Signals are used to analyse the pulse widths (Abu-Rub, Haitham, Iqbal and Guzinski,2021). The PWM is a sine function. If the sine wave magnitude is more than a triangle wave, the upper key is active, otherwise, the corresponding phase and the lower switch open. Less harmonic output is generated with sinusoidal PWM compared to square wave converter. The frequency varies according to the index of modulation. Harmonics occurring at the output are at high frequency. The frequency index of modulation raises the harmonic, and the spectrum rises to a higher frequency and can be filtered by a simple method.

A decoupled d-q solution is a simplified control method using a PWM voltage-adjusted scheme which is commonly used in the wind energy sector and many other clean energy systems. Temporary simulation or transient calculation techniques typically test control system efficiency. Usually, power quality is not a criterion to be considered while designing controllers in terms of unbalances and harmonics (Li, Shuhui and Ling Xu, 2008). A full-wave 3-phase adjuster for RSC and GSC and a three-phase, three-level with an insulated bipolar gate transistors (IGBTs) are used in the wind turbine. The PWM modulation technique is used to produce IGBT gate pulses. This approach modulates the input reference AC signal to a high frequency and eliminates disruptive low-frequency harmonics by using a high-frequency carrier signal.

3.2. Analytic Model Background

The mathematical method applied in this thesis is given in this chapter.

3.2.1. Phase Machine Model

The phase mechanical model is investigated under two sub-topics: generator electrical and mechanical equations.

In, the equivalent circuit of DFIG is given on the d-q reference axis, rotating at synchronous speed.

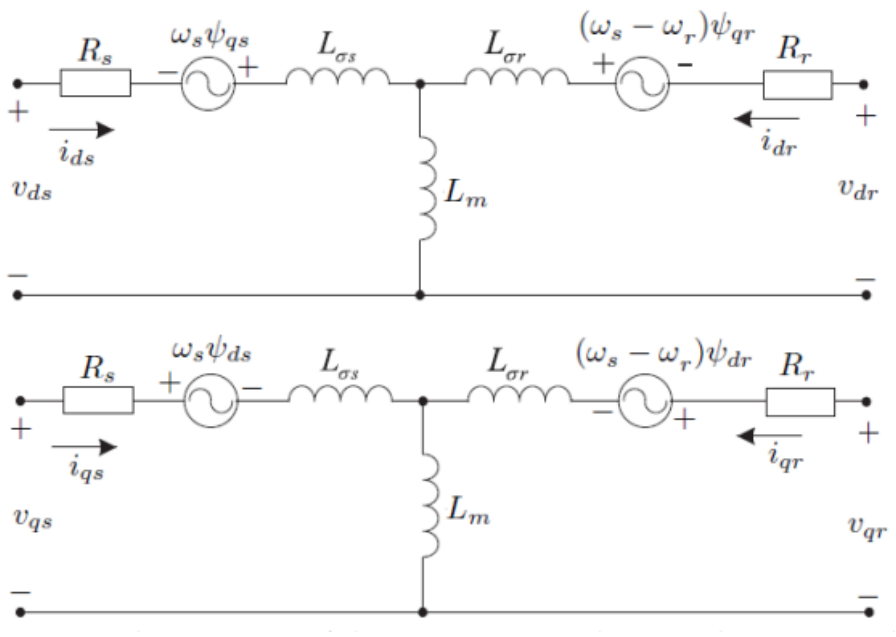

Figure 7. Shows an approximate frequency domain circuit model of the 3-phase DFIG.

For stator and rotor voltages from the DFIG equivalent circuit, equations (3.1) - (3.4) were constructed.

$$v_{ds} = R_s i_{ds} + L_s \frac{di_{ds}}{dt} - w_s \psi_{qs} + L_m \frac{di_{dr}}{dt} \quad (3.1)$$

$$v_{ds} = R_s i_{ds} + L_s \frac{di_{ds}}{dt} - w_s \psi_{qs} + L_m \frac{di_{dr}}{dt} \quad (3.2)$$

$$v_{dr} = R_r i_{dr} + L_r \frac{di_{dr}}{dt} - (w_s - w_r)\psi_{qr} + L_m \frac{di_{ds}}{dt} \quad (3.3)$$

$$v_{qr} = R_r i_{qr} + L_r \frac{d_{iqr}}{dt} + (w_s - w_r)\psi_{dr} + L_m \frac{di_{qs}}{dt} \quad (3.4)$$

Equations (3.5) and (3.8) represent the stator flux linkages and rotor flux linkages in terms of self-inductances.

$$\psi_{ds} = L_s i_{ds} + L_m i_{dr} \quad (3.5)$$

$$\psi_{qs} = L_s i_{qs} + L_m i_{qr} \quad (3.6)$$

$$\psi_{dr} = L_r i_{dr} + L_m i_{ds} \quad (3.7)$$

$$\psi_{qr} = L_r i_{qr} + L_m i_{qs} \tag{3.8}$$

In Equations (3.9) and (3.10), the stator (L_s) and rotor (L_r) self-inductances are defined as the sum of the magnetizing inductance and the stator and rotor leakage inductances.

$$L_s = L_m + L_{\sigma s} \tag{3.9}$$

$$L_r = L_m + L_{\sigma r} \tag{3.10}$$

The mechanical dynamics of the system can be written for DFIG as in equation (3.11).

$$\frac{d_{wm}}{dt} = \frac{1}{J}(T_m - T_e - Bw_m) \tag{3.11}$$

The equation for the relationship between rotor mechanical angular speed w_m and rotor angular speed w_r is provided in the equation (3.12)

$$w_r = w_s - pw_m \tag{3.12}$$

Where p is the number of DFIG pole pairs. The electromagnetic torque and total stator active and reactive power are calculated using equations (3.13) and (3.15) for stator and rotor currents and voltages.

$$\mathrm{T_e} = \frac{3}{2} p L_m (\ i_{dr}\ i_{qs} - \ i_{qr} i_{ds}) \tag{3.13}$$

$$P_S=\frac{3}{2}(v_{ds}\, i_{ds} + v_{qs} i_{qs}) \tag{3.14}$$

$$Q_S=\frac{3}{2}(v_{qs}\, i_{ds} - v_{ds} i_{qs}) \tag{3.15}$$

DFIGs typically run at 30% of the generator's synchronous speed. The generator's ability to be regulated within this range is determined by the generator's slip rate. Equation (3.16) gives the generic slip expression (s) for induction devices.

$$s=\frac{w_s - p w_m}{w_s} = \frac{w_r}{w_s} \tag{3.16}$$

In Equation (3.17), the slip expression is defined as the ratio of the frequency of the rotor currents (f_r) to the frequency of the stator currents (f_s).

$$s=\frac{f_r}{f_s} \tag{3.17}$$

The angular speed of the stator field is constant. As a result, the slip may be adjusted based on the angular speed of the rotor field. Equation (3.18) is used to explain the conversion of mechanical power to electrical power in induction devices.

$$P_m = P_S + P_r \tag{3.18}$$

Where P_m, P_S, and P_r denote the total mechanical power in the generator shaft, the electrical power received from the stator, and the power received or given from the rotor. The total power generated by the stator and rotor is known as turbine power. Equations (3.19) define the power expression in terms of the torque equation.

$$T_m w_s = T_m w_r - P_r \tag{3.19}$$

T_m denotes the mechanical torque of a wind turbine. The rotor power (P_r) can be expressed by rewriting Equation (3.18), as illustrated in Equations (3.20).

$$P_r = -T_m(w_s - w_r) \tag{3.20}$$

$$P_r = -sT_m w_s = -P_S \tag{3.21}$$

Rotor active and reactive powers are defined using Equations (3.22) and (3.23), respectively.

$$P_r = \frac{3}{2}(v_{dr}\, i_{dr} + v_{qr} i_{qr}) \tag{3.22}$$

$$Q_S = \frac{3}{2}(v_{qr}\, i_{dr} - v_{dr} i_{qr}) \tag{3.23}$$

3.2.1.1. Generator Electrical Equation

In Figure 8 the rotor and stator winding layouts for DFIG are given.

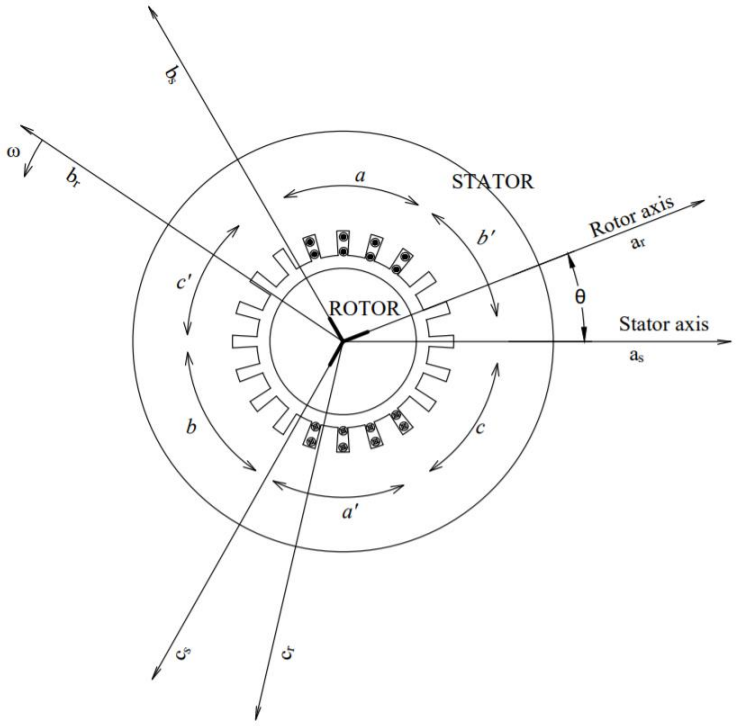

Figure 8. ϕ machine cross-section

Table 1.Shows the parameters and electrical magnitude most representative of the model are:

Stator and Rotor Electrical Parameters	**Stator and Rotor Electrical Magnitudes**
$\boldsymbol{L^{\sigma s}}$: Stator leakage inductance (H)	$\mathbf{v^s}$: Supplied stator voltage
$\boldsymbol{L^{\sigma r}}$: Rotor leakage inductance (H)	$\mathbf{v^r}$**:** Supplied rotor voltage
$\boldsymbol{L^m}$: Mutual inductance (H)	$\mathbf{I^s}$: Stator current
$\boldsymbol{R^s}$: Stator resistance (Ω)	$\mathbf{I^r}$: Rotor current
$\boldsymbol{R^r}$: Rotor resistance (Ω)	
$\boldsymbol{L^{sr}}$: Amplitude of the inductance matrix	
$\boldsymbol{\theta_r}$: Instantaneous angle difference between stator and rotor axes	
Ns, Nr: Number of turns per phase for stator and rotor windings	

The 3-phase electrical dynamical equations for the rotor and stator are shown by equations (3.24) and (3.25).

$$v^s_{abc} = R^s * i^s_{abc} + \frac{d}{dt}\psi^s_{abc} \tag{3.24}$$

$$v^r_{abc} = R^r * i^r_{abc} + \frac{d}{dt}\psi^r_{abc} \tag{3.25}$$

The superscript "r" in the equations the rotor is represented by, and the superscript "s" represents the stator. The expression" ψ" stands for the flux formed in a winding. "ψ" is formed by multiplying the inductance value in the generator windings with the current.

$$\psi = L * i \tag{3.26}$$

The flux expression " ψ" is expressed by equation (3.27) in stator and rotor circuits for a 3-phase machine.

$$\begin{bmatrix} \psi^s_{abc} \\ \psi^r_{abc} \end{bmatrix} = \begin{bmatrix} [L^s] & [L^{sr}] \\ [L^{sr}]^T & [L^r] \end{bmatrix} \begin{bmatrix} i^s_{abc} \\ i^r_{abc} \end{bmatrix} \tag{3.27}$$

The inductance matrix is:

$$[L^s] = \begin{bmatrix} L^{\sigma s} + L^{ms} & -\frac{1}{2}L^{ms} & -\frac{1}{2}L^{ms} \\ -\frac{1}{2}L^{ms} & L^{\sigma s} + L^{ms} & -\frac{1}{2}L^{ms} \\ -\frac{1}{2}L^{ms} & -\frac{1}{2}L^{ms} & L^{\sigma s} + L^{ms} \end{bmatrix} \tag{3.28}$$

$$[L^r] = \begin{bmatrix} L^{\sigma r} + L^{mr} & -\frac{1}{2}L^{mr} & -\frac{1}{2}L^{mr} \\ -\frac{1}{2}L^{mr} & L^{\sigma r} + L^{mr} & -\frac{1}{2}L^{mr} \\ -\frac{1}{2}L^{mr} & -\frac{1}{2}L^{mr} & L^{\sigma r} + L^{mr} \end{bmatrix} \tag{3.29}$$

The inductance values of the windings on the stator and rotor are irrespective of the rotor position of the machine's rotating part. They are constant values based on where the rotor is located.

The inductance matrix's value depends on the rotor's rotation among the stator's and rotor's windings. This situation is shown by equation (3.30).

$$[L^{sr}] = L^{sr} \begin{bmatrix} cos(\theta_r) & cos\left(\theta_r + \frac{2\pi}{3}\right) & \cos\left(\theta_r - \frac{2\pi}{3}\right) \\ cos\left(\theta_r - \frac{2\pi}{3}\right) & cos(\theta_r) & \cos\left(\theta_r + \frac{2\pi}{3}\right) \\ cos\left(\theta_r + \frac{2\pi}{3}\right) & cos\left(\theta_r - \frac{2\pi}{3}\right) & \cos\left(\theta_r\right) \end{bmatrix} \tag{3.30}$$

The stator axis is fixed, and the rotor axis rotates, so angle θ_r changes proportionally with rotor rotation speed. Flux (ψ) is calculated by substituting (3.30) and (3.31) in equation (3.27).

$$\begin{bmatrix}\psi as\\ \psi bs\\ \psi cs\\ \psi ar\\ \psi br\\ \psi cr\end{bmatrix}=\begin{bmatrix} L^{\sigma s}+L^{ms} & -\frac{1}{2}L^{ms} & -\frac{1}{2}L^{ms} & & & \\ -\frac{1}{2}L^{ms} & L^{\sigma s}+L^{ms} & -\frac{1}{2}L^{ms} & & [\ L^{sr}\ ] & \\ -\frac{1}{2}L^{ms} & -\frac{1}{2}L^{ms} & L^{ms}+L^{ms} & & & \\ & & & L^{\sigma r}+L^{mr} & -\frac{1}{2}L^{mr} & -\frac{1}{2}L^{mr} \\ & & & -\frac{1}{2}L^{mr} & L^{\sigma r}+L^{mr} & -\frac{1}{2}L^{mr} \\ & & & & & \end{bmatrix} \quad (3.31)$$

While it is written the inductance matrix obtained in (3.31) in (3.24) in addition to the flux expression in the generator's stator and rotor dynamic equations circuits written in (3.25), the equation (3.32) is obtained.

$$\begin{bmatrix}vas(t)\\ vbs(t)\\ vcs(t)\\ var(t)\\ vbr(t)\\ vcr(t)\end{bmatrix}=\begin{bmatrix}rs&0&0&0&0&0\\ 0&rs&0&0&0&0\\ 0&0&rs&0&0&0\\ 0&0&0&rr&0&0\\ 0&0&0&0&rr&0\\ 0&0&0&0&0&rr\end{bmatrix}*\begin{bmatrix}ias(t)\\ ibs(t)\\ ics(t)\\ iar(t)\\ ibr(t)\\ icr(t)\end{bmatrix}+\frac{d}{dt}\left(\begin{bmatrix}L^{s}(\theta(t)) & L^{sr}(\theta(t))\\ L^{srT}(\theta(t)) & L^{r}(\theta(t))\end{bmatrix}*\begin{bmatrix}ias(t)\\ ibs(t)\\ ics(t)\\ iar(t)\\ ibr(t)\\ icr(t)\end{bmatrix}\right) \quad (3.32)$$

In the most general form, the electrical dynamics equations of the generator (3 phases) are obtained. Depending on the stator and rotor, 6 dynamic electrical equations are written. When expressed as a function of inductance and matrices, the flux, current, and inductance are not fixed values. Instead, they vary with time. The current changes over time and the inductance are calculated by applying the derivative of the flux value with respect to its variation with θ. The matrices involved in these calculations are not constant and can also vary. Since solving the product derivative expression in matrix form is complex, a simpler model for solving electrical dynamics equations will be used in the following sections.

3.2.1.2. Generator Mechanical Equation

While obtaining mechanical dynamical equations, the equations vary depending on the generator or engine operation of the machine. The moment given to the machine is of a negative sign, and the moment taken from the machine is of a positive sign. Therefore, in generator operation, the mechanical dynamical equation is as in (3.33).

$$[T_e] - [T_m] = J * \frac{dw}{dt} + B * w \tag{3.33}$$

Electromagnetic and mechanical moment generated in the generator with equation (3.33), the difference between the values of the generator depends on the inertia of the generator and the friction coefficient. It is seen that the rotor changes the angular rotation speed.

$$T_{e\,=p*(i^s_{abc})^T} * \frac{d[L_{sr}]}{d\theta} * (i^r_{abc}) \tag{3.34}$$

The common inductance matrix current and θ are variable. With this interaction, an electromagnetic moment is formed (3.34). The electromagnetic torque calculation given for the three-phase machine model is quite complex, as is the calculation of the electrical dynamic equations.

3.2.3. Axis Transformations

Complex solutions of 3-phase generator electrical and mechanical dynamical equations have been mentioned before. To facilitate these solutions, Clarke transformations were found by Edith Clarke. With this approach, the machine model shown as 3 phases have been reduced to 2 phases. Later, it was developed with Park transformations and the rotor axis. Axes rotating together with the axis set to dq axes, obtained in αβ axes transformed the machine model. In the park transformation, dq

rotating with rotor axes the rotor of the machine variables obtained by assigning machine variables to the axes position dependency is eliminated. Thus, in the dq axes, the resulting solution of machine dynamical equations becomes simpler. Krause transforms are directly from the three-phase machine model in matrix form to the dq axis allowing switching to the machine model.

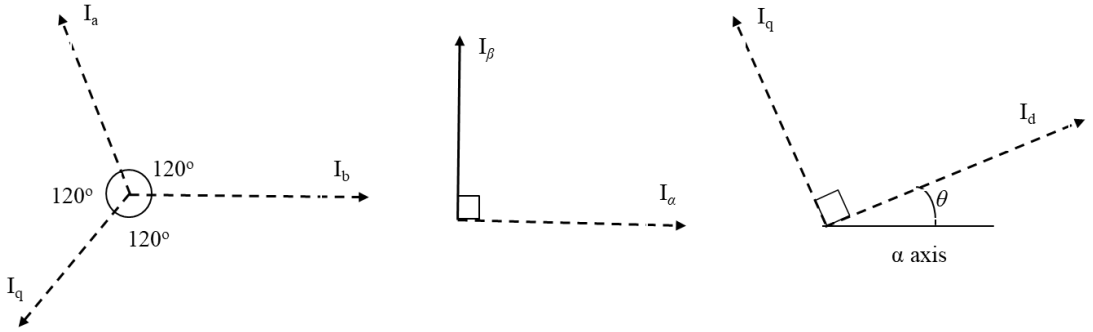

Figure 9. Reference frame of parking transformation

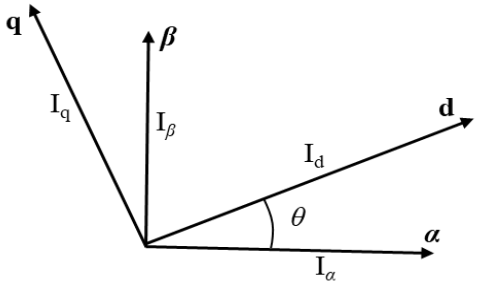

Figure 10. Park transformation vector diagram.

$$I\alpha = I\alpha$$
$$I\beta = \frac{1}{\sqrt{3}} * I\alpha + \frac{2}{\sqrt{3}} I\beta \quad (3.34)$$
$$I\alpha + I\beta + Ic = 0$$

Equation (3.34) ABC stator machine model in stationary axis set and stationary αβ expresses the relationship between the axis set.

3.2.4. Vector Representation

Park transformation equations, shown equations with (3.35) and (3.36).

$$Id = Ia*\cos(\theta) + I\beta*\sin(\theta) \tag{3.35}$$

$$Iq = -I\alpha *\sin(\theta) + I\beta*\cos(\theta) \tag{3.36}$$

With the Clarke transform, the machine model is passed from three-phase to two-phase stationary axes (αβ) and then with the parking transformation equations given by (3.35) and (3.36), the αβ axes set. The machine model is reduced to the dq axes, which are the rotating axes. As a result, the stationary axis in 3-phase from the set the rotating axis to 2-phases. Clarke and Park transform equations with the dq axis model finalized by Krause arranged from the three-phase machine model to the dq rotating axis set machine model. The transition matrix and likewise three-phase axis from the dq axis set inverse transformation matrix, stator, and rotor dq with stator and rotor axes to reduce variables to dq axes. The instantaneous angle value(Θ) between the axes is used in the transformation taking place.

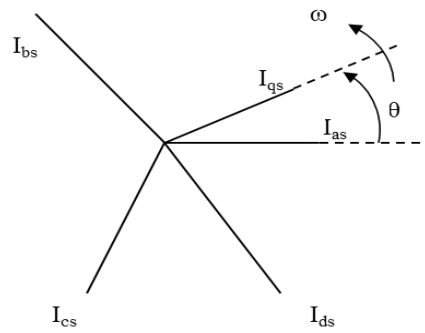

Figure 11. Stator and dq axes vector diagram

$$[I^s_{qd0}] = K^s * [I^s_{abc}] \tag{3.37}$$

$$\left(I_{qd0}\right)^T = [Iqs\ Ids\ Ios] \tag{3.38}$$

$$[K^s] = \frac{2}{3}\begin{bmatrix} cos(\theta) & cos\left(\theta - \frac{2\pi}{3}\right) & \cos\left(\theta + \frac{2\pi}{3}\right) \\ sin(\theta) & \sin\left(\theta - \frac{2\pi}{3}\right) & \sin\left(\theta - \frac{2\pi}{3}\right) \\ \frac{1}{2} & \frac{1}{2} & \frac{1}{2} \end{bmatrix} \tag{3.39}$$

$$[K^s]^{-1} = \begin{bmatrix} cos(\theta) & sin(\theta) & 1 \\ cos\left(\theta - \frac{2\pi}{3}\right) & \sin\left(\theta - \frac{2\pi}{3}\right) & 1 \\ \cos\left(\theta + \frac{2\pi}{3}\right) & \sin\left(\theta + \frac{2\pi}{3}\right) & 1 \end{bmatrix} \tag{3.40}$$

$$\theta = \int w dt + c \tag{3.41}$$

In the three-phase machine model above, the stator stationary axes variables choose the dq axis set using the angle θ between the axes, using the $[K^s]$ matrix given in (3.39) and the inverse transformation matrix given in (3.40), the variables expressed in the dq axis set using $[K^s]^{-1}$.The three-phase stator is reduced to the stationary axis set.

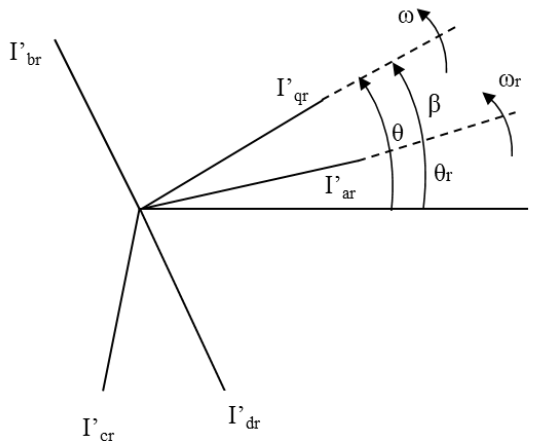

Figure 12. Rotor and dq axes vector diagram.

$$[I'^{r}_{qd0}] = K^{r} * [I'^{r}_{abc}] \tag{3.42}$$

$$\left(I'^{r}_{qd0}\right)^{T} = [I'qr\ I'dr\ I'or] \tag{3.43}$$

$$[K^{r}] = \frac{2}{3}\begin{bmatrix} cos(\beta) & cos\left(\beta - \frac{2\pi}{3}\right) & \cos\left(\beta + \frac{2\pi}{3}\right) \\ sin(\beta) & \sin\left(\beta - \frac{2\pi}{3}\right) & \sin\left(\beta - \frac{2\pi}{3}\right) \\ \frac{1}{2} & \frac{1}{2} & \frac{1}{2} \end{bmatrix} \tag{3.44}$$

$$[K^{r}]^{-1} = \begin{bmatrix} cos(\beta) & sin(\beta) & 1 \\ cos\left(\beta - \frac{2\pi}{3}\right) & \sin\left(\beta - \frac{2\pi}{3}\right) & 1 \\ \cos\left(\beta + \frac{2\pi}{3}\right) & \sin\left(\beta + \frac{2\pi}{3}\right) & 1 \end{bmatrix} \tag{3.45}$$

$$\beta = \theta - \theta r \Rightarrow \theta r = \int wr\, dt + c \tag{3.46}$$

In the above three-phase machine model the rotor axis variables are set to the dq axis with the β angle between axials, with the matrix $[Kr]$ indicated in (3.44) and the dq axis set, with the inverted transformation matrix $[Kr]^{-1}$ indicated in the above-mentioned model (3.45). The rotating axis reduces the three-phase rotor.

$$i'^{r}_{abc} = \frac{N_r}{N_s} i^{r}_{abc} \tag{3.47}$$

$$v'^{r}_{abc} = \frac{N_s}{N_r} v^{r}_{abc} \tag{3.48}$$

$$\psi'^{r}_{abc} = \frac{N_s}{N_r} \psi^{r}_{abc} \tag{3.49}$$

$$L'^{sr} = \frac{N_s}{N_r} L^{sr} = L^{ms} \tag{3.50}$$

$$L^{mr} = \left(\frac{N_r}{N_s}\right)^2 L^{ms} = L'^{r} = L'^{\sigma r} + L^{ms} \tag{3.51}$$

3.2.5. Dq Axis Set Mathematical Model

Dq axis of stator variables stator for three phases given in (3.24) $[Ks]$transformation matrix is applied to the equation belonging to the circuit. The Axis for the resistance and flux variables that transform the voltage applies because the voltage expression in (3.24) results from the interaction of resistance and current. It is equivalent to the total of the voltage values from the formed and flux expression. If dq conversion is made for the voltage value caused by the resistor circuit elements.

$$[v^{s}_{abc}] = [R^{s}] * [\, i^{s}_{abc}] \tag{3.52}$$

$$[K^s]^{-1}*[v^s_{qd0}]= [R^s] * [K^s]^{-1}*[i^s_{qd0}] \quad (3.53)$$

When the matrix is multiplied by both sides of the equation $[K^s]$, the expression $[\ v^s_{qd0}]$ is left alone and equation (3.54) is obtained.

$$[K^s] * [K^s]^{-1}*[\ v^s_{qd0}]= [K^s] * [R^s] * [K^s]^{-1}*[i^s_{qd0}] \quad (3.54)$$

Equation (3.54) is simplified, and general equation (3.55) is formed.

$$[\ v^s_{qd0}]=[\ R^s_{qd0}]*[\ i^s_{qd0}] \quad (3.55)$$

Since $[\ R^s_{qd0}]=[\ K^s]*[\ R^s]*\ [K^s]^{-1}$ the resistance matrix used for the 3-phase generator is used in the dq axis mathematic model.

$$\left[R^s_{qd0}\right] = \begin{bmatrix} rs & 0 & 0 \\ 0 & rs & 0 \\ 0 & 0 & rs \end{bmatrix} \quad (3.56)$$

Considering the flux when dq conversion is made for the voltage value.

$$[v^s_{abc}] = \frac{d}{dt}[\psi^s_{abc}] \quad (3.57)$$

$$[K^s]^{-1} * \left[v^s_{qd0}\right] = \frac{d}{dt}\left([K^s]^{-1} * \left[\psi^s_{qd0}\right]\right) \quad (3.58)$$

Equations depending on the flux are obtained. If the equation's two sides are multiplied by $[K^s]$, $[v_{qd0}^s]$ is left alone and the following equations are obtained.

$$[K^s] * [K^s]^{-1} * \left[v_{qd0}^s\right] = \frac{d}{dt}\left([K^s]^{-1} * \left[\psi_{qd0}^s\right]\right) \tag{3.59}$$

$$\left[v_{qd0}^s\right] = [K^s] * \left[\left(\frac{d}{dt}[K^s]^{-1} * \left[\psi_{dq0}^s\right]\right) + \left([K^s]^{-1} * \frac{d}{dt}\left[\psi_{dq0}^s\right]\right)\right] \tag{3.60}$$

$$\left[v_{qd0}^s\right] = \left[\left([K^s] * \frac{d}{dt}\left([K^s]^{-1} * \left[\psi_{dq0}^s\right]\right)\right) + \left([K^s] * [K^s]^{-1} * \frac{d}{dt}\left[\psi_{dq0}^s\right]\right)\right] \tag{3.61}$$

From here;

$$\frac{d}{dt}[K^s]^{-1} = w* \begin{bmatrix} -sin(\theta) & cos(\theta) & 0 \\ -sin\left(\theta - \frac{2\pi}{3}\right) & \cos\left(\theta - \frac{2\pi}{3}\right) & 0 \\ -sin\left(\theta + \frac{2\pi}{3}\right) & \cos\left(\theta + \frac{2\pi}{3}\right) & 0 \end{bmatrix} \tag{3.62}$$

$$[K^s] * \frac{d}{dt}[K^s]^{-1} = w * \begin{bmatrix} 0 & 1 & 0 \\ -1 & 0 & 0 \\ 0 & 0 & 0 \end{bmatrix} \tag{3.63}$$

equations are obtained. If (3.41) is substituted in (3.61), it is obtained (3.64).

$$\left[v_{qd0}^s\right] = w*\left[\psi_{qd0}^s\right] + \frac{d}{dt}\left[\psi_{qd0}^s\right] \tag{3.64}$$

$$\left[v_{qd0}^s\right] = [vqs \quad vds \quad vos]^T \tag{3.65}$$

$$\left[\psi_{qd0}^{s}\right] = [\psi ds \;\; - \;\; \psi qs \;\;\; \psi os] \tag{3.66}$$

For the voltage equations in the dq axis set consisting of the flux, the equations (3.64) and (3.66) are written in the expression (3.64) the following equations are obtained.

$$vqs = w * \psi ds + \frac{d}{dt}\psi qs \tag{3.67}$$

$$vds = -w * \psi qs + \frac{d}{dt}\psi ds \tag{3.68}$$

$$vos = \frac{d}{dt}\psi os \tag{3.69}$$

If the resistance voltage expressions and flux expressions are written together, the general voltage equations are obtained from the stator's dq axis set.

$$vqs = rs * iqs + w * \psi ds + \frac{d}{dt}\psi qs \tag{3.70}$$

$$vds = rs * ids - w * \psi qs + \frac{d}{dt}\psi ds \tag{3.71}$$

$$\mathrm{vos} = \mathrm{rs} * \mathrm{ios} + \frac{\mathrm{d}}{\mathrm{dt}}\psi \mathrm{os} \tag{3.72}$$

To know the voltage values caused by the flux in equations (3.70), (3.71) and (3.72), the inductance matrices in the dq axis set of the stator circuit must be known. The following equations are obtained by transforming the matrix to the dq axis set.

$$[\psi_{abc}^{s}] = [L^{s}] * [i_{abc}^{s}] \tag{3.73}$$

$$[K^s]^{-1} * \left[\psi^s_{qd0}\right] = [L^s] * [K^s]^{-1} * \left[i^s_{qd0}\right] \tag{3.74}$$

If the two sides of the equation are multiplied from the left by the matrix $[K^s]$, leaving the expression $[\left[\psi^s_{qd0}\right]]$ alone, it becomes as follows.

$$[K^s] * [K^s]^{-1} * \left[\psi^s_{qd0}\right] = [K^s] * [L^s] * [K^s]^{-1} * \left[i^s_{qd0}\right] \tag{3.75}$$

When the equation (3.53) is arranged, the expression (3.54) is obtained.

$$\left[\psi^s_{qd0}\right] = \left[L^s_{qd0}\right] * \left[i^s_{qd0}\right] \tag{3.76}$$

$$\left[L^s_{qd0}\right] = [K^s] * [L^s] * [K^s]^{-1} \tag{3.77}$$

The inductance matrix of the stator is;

$$[L^s] = \begin{bmatrix} L^{\sigma s} + L^{ms} & -\frac{1}{2}L^{ms} & -\frac{1}{2}L^{ms} \\ -\frac{1}{2}L^{ms} & L^{\sigma s} + L^{ms} & -\frac{1}{2}L^{ms} \\ -\frac{1}{2}L^{ms} & -\frac{1}{2}L^{ms} & L^{\sigma s} + L^{ms} \end{bmatrix} \tag{3.78}$$

When the expression $[L^s]$ is replaced in (3.55) the inductance matrix of the stator in the dq axis set is obtained.

$$\left[L^s_{qd0}\right] = \begin{bmatrix} L^{\sigma s} + \frac{3}{2}L^{ms} & 0 & 0 \\ 0 & L^{\sigma s} + \frac{3}{2}L^{ms} & 0 \\ 0 & 0 & L^{\sigma s} \end{bmatrix} \tag{3.79}$$

The stator's inductance matrix is obtained in the dq axis set, and the rotor circuit and the in the dq axis set are obtained equation (3.59) (3.60), respectively.

$$\begin{bmatrix} \psi^{s}_{qd0} \\ \psi'^{s}_{qd0} \end{bmatrix} = \begin{bmatrix} [K^s]*[L^s]*[K^s]^{-1} & [K^s]*[L^{sr'}]*[K^r]^{-1} \\ [K^r]*[L^{sr'}]*[K^s]^{-1} & [K^r]*[L^{r'}]*[K^r]^{-1} \end{bmatrix} * \begin{bmatrix} i^{s}_{qd0} \\ i'^{r}_{qd0} \end{bmatrix} \quad (3.80)$$

$$[K^s]*[L^s]*[K^s]^{-1} = \left[L^{s}_{qd0}\right] = \begin{bmatrix} L^{\sigma s} + \frac{3}{2}L^{ms} & 0 & 0 \\ 0 & L^{\sigma s} + \frac{3}{2}L^{ms} & 0 \\ 0 & 0 & L^{\sigma s} \end{bmatrix} \quad (3.81)$$

$$[K^r]*[L^{r'}]*[K^r]^{-1} = \left[L^{r}_{qd0}\right] = \begin{bmatrix} L^{\sigma r} + \frac{3}{2}L^{ms} & 0 & 0 \\ 0 & L^{\sigma r'} + \frac{3}{2}L^{ms} & 0 \\ 0 & 0 & L^{\sigma r'} \end{bmatrix} \quad (3.82)$$

With Equation (3.60) the inductance matrix was created for the rotor.

$$[K^s]*[L^{sr'}]*[K^r]^{-1} = [K^r]*[L^{sr'}]^{T}*[K^s]^{-1} = \left[L^{sr}_{qd0}\right] \quad (3.83)$$

$$\left[L^{sr}_{qd0}\right] = \begin{bmatrix} \frac{3}{2}L^{ms} & 0 & 0 \\ 0 & \frac{3}{2}L^{ms} & 0 \\ 0 & 0 & 0 \end{bmatrix} \quad (3.84)$$

The inductance matrix in the dq axis set is formed via the interaction of the stator and rotor. In addition, if the 0s are not considered in the matrix, the dimensions of the matrix decrease from 6x6 to 4x4 and thus provide the desired convenience in solving generator dynamic equations. When the necessary transformations are applied, the generator dynamic equations (for voltage and flux) in their most general form are as follows.

$$vqs = rs*iqs + w*\psi ds + \frac{d}{dt}\psi qs \tag{3.85}$$

$$vds = rs*ids - w*\psi qs + \frac{d}{dt}\psi ds \tag{3.86}$$

$$vos = rs*ids + \frac{d}{dt}\psi os \tag{3.87}$$

$$v'qr = r'r*i'qr + (w - wr)*\psi'dr + \frac{d}{dt}\psi' qr \tag{3.88}$$

$$v'dr = r'r*i'dr - (w - wr)*\psi'qr + \frac{d}{dt}\psi' dr \tag{3.89}$$

$$v'or = r'r*i'qr + \frac{d}{dt}\psi' or \tag{3.90}$$

$$\psi qs = L^{\sigma s}*iqs + \frac{3}{2}\ L^{ms}(iqs + i'qr) \Rightarrow \psi qs = L^{s}*iqs + \ L_M*i'qr \tag{3.91}$$

$$\psi ds = L^{\sigma s}*ids + \frac{3}{2}\ L^{ms}(ids + i'dr) \Rightarrow \psi ds = L^{s}*ids + \ L_M*i'dr \tag{3.92}$$

$$\psi os = L^{\sigma s}*ios \tag{3.93}$$

$$\psi' qr = L'^{\sigma r}*i'qr + \frac{3}{2}\ L^{ms}(iqs + i'qr) \Rightarrow \psi' qr = L'^{r}*iq'r + \ L^{m}*iqs \tag{3.94}$$

$$\psi' dr = L'^{\sigma r}*i'dr + \frac{3}{2}\ L^{ms}(ids + i'dr) \Rightarrow \psi' dr = L'^{r}*i'dr + \ L^{m}*ids \tag{3.95}$$

$$\psi' or = L'^{\sigma r}*i'0r \tag{3.96}$$

$$L_M = \frac{3}{2}\ L^{ms} \tag{3.97}$$

Similarly, in mechanical equations, the following general equations are obtained.

$$T_e = p*[K^s]^{-1}*i^s_{qd0}]^T * \frac{d[L^{sr}{}_I]}{d\theta}*\left[\left[K^{r-1}\right] * \left(i'^r_{qd0}\right)'\right] \quad (3.98)$$

The most regular form of the electromagnetic torque expression on the dq axis is given by equation (3.99).

$$T_e = \left(\frac{3}{2}\right)*p*L_M*(iqs*i'dr - ids*i'qr) \quad (3.99)$$

Different types of electromagnetic torque expressions depending on flux areas in equation (3.100) and (3.101).

$$T_e = \left(\frac{3}{2}\right)*p*(\psi'qr*i'dr - \psi dr*i'qr) \quad (3.100)$$

$$T_e = \left(\frac{3}{2}\right)*p*(\psi ds*iqs-\psi qs*ids) \quad (3.101)$$

Thus, the general electrical and mechanical equations for the generator were obtained in their simplest form by applying Clark and Park and then Krause transformations. A mathematical basis was created for the Dfig modelling and control, which will be done in the next section.

3.3. Simulation Design of Dfig

For a partial-scale wind turbine has back-to-back power converter with a doubly fed asynchronous generator, the control stages with a field-oriented vector control method Figure 14 will be explained in detail in this section.

3.3.1. Dfig System Control Modelling

With the vector control method, controllers that cannot be operated at PID or other high frequencies can be operated. The higher frequency, the lower the performance of the PID controllers and the phase and voltage values deviate from the reference value. AC motors are modelled as DC and when DC signals are applied to the linear controller thus, efficient control is achieved. Dq transformations are the basis of the vector control method. Furthermore, the DC structure of these variables obtained from the dq axis set simplifies the control algorithm and converts it into a control structure accomplished in a direct current machine. The dq axis and DC components are produced by transforming the three-phase current variables with transform matrices. A stator and the rotor's magnetic field are regulated independently of one another using these current components. The generator model is always obtained in the dq axes because the vector control approach is dependent on them. The current information received from the induction motor is reduced from 3 phases to 2 phases by the Clark transform. The Clark transform stator currents with a phase difference of 120 degrees between them are converted into currents with a phase difference of 90 degrees between them. These currents are converted to DC quantities by Park transformation. DC signals are sent to linear regulators and pass through the controller with bearing (position angle). After this stage, 2 sinusoidal signals with phase differences are formed between them with the reverse parking transformation. These signals ingress to PWM, and converter switching takes place. Thus, the field-directed vector control operation is performed Figure 14.

A DFIG converter controls a study in two parts: the grid and the rotor side. The RSC controls the generator's reactive and active power using IGBT gate signals, while the GSC adjusts the DC Link voltage amplitude using IGBT gate signals.

3.3.1.1. Control of RSC

The position of the stator flux vector of the doubly fed asynchronous generator is controlled by aligning it with the q-axis and using a synchronously rotating reference frame. Thus, the three-phase axis set is reduced to the dq axis set and the active and reactive powers on the stator side can be controlled separately. The space vector shows the relationship between the stationary reference frame and the stator flux reference frame.

By using an RSC, controlling the generator's output of both active and reactive power is feasible. For the RSC, the dq axis's angular rotation speed is set is selected as equivalent to the grid voltage's angular speed. By applying stator flux orientation to the generator model created the machine's active and reactive power are considered separate from one another. The converter on the RSC provides power generation thanks to the frequency change depending on the slip ring on the rotor.

3.3.1.2. Control of GSC

The purpose of the grid side converter control is to control the DC-link voltage and to provide reactive power to the grid when needed. In grid side converter control, the three-phase system is reduced to two-phase (dq-axes) using the vector control method (stator voltage orientation). One control variable with each set of axes Is controlled. The vector diagram of the DQ synchronous reference frame for the GSC converter is given in Figure 13. The synchronous reference frame is parallel to the d-axis reference frame. When the q component of the voltage is zero, the d component equals the grid voltage. The DC link voltage is managed using the d-axis component in the DQ axis set, while reactive power support to the grid is adjusted with the q -axis component as needed.

$$v_{dr} R_r i_{dr} + \sigma L_r \frac{d}{dt} i_{dr} \omega_r \sigma L_r i_{qr} + \frac{L_m}{L_s} \frac{d}{dt} |\psi_s| \tag{3.102}$$

$$v_{qr} = R_r i_{qr} + \sigma L_r \frac{d}{dt} i_{qr} - \omega_r \sigma L_r i_{dr} + \omega_r \frac{L_m}{L_s} |\psi_s| \tag{3.103}$$

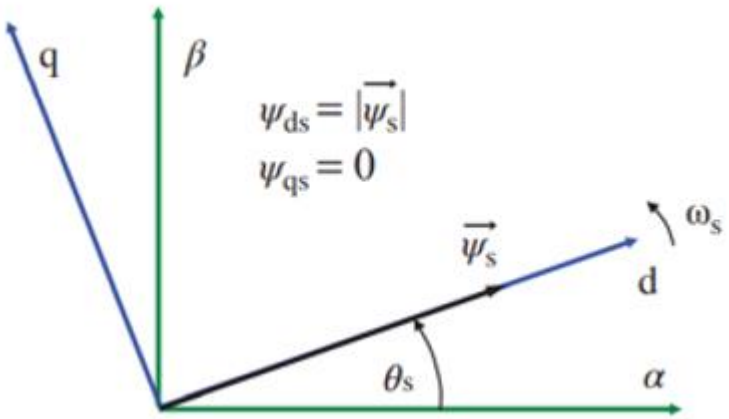

Figure 13. Depicts a synchronous spinning aligned with the stator flow vector for dq in the reference frame.

A constant AC voltage and direct connection to the power source cause a minimal voltage to drop across the stator resistance and a steady stator flux, so that, $d|\psi_s|$/dt is zero. The two subsequent equations demonstrate that it is possible to control d_q rotor current for each current component using a regulator. To estimate the stator flux and ω_r, the cross terms of equation (3.77) are included in the output of the regulators to assist the regulator. Angle Θ_r must be estimated for the transformation of the reference frame. First, Control must be taken for d_q coordinates, rotor currents and voltages must then DQ coordinates were converted. Current loops in the control chart run using rotor currents as they relate to conversion to rotor-referenced values on the stator side happen during the measuring step for currents and before the converter generates pulses for voltages.

Vector control of GSC, the angular rotation speed of the dq axis set is selected as equivalent to the grid's angular speed voltage. The responsibility of the GSC is to control the electricity going from the rotor's windings to the grid, both active and reactive or from the grid to the windings, independent of the power flow direction. The converter on the grid side provides power generation at the stator output thanks to the DC link.

3.3.1.3. Control Loops for Power and Speed

By analysing the control loops and determining the flux angle, the complete control system can be examined. The torque measured in the dq frame perhaps concisely written as follows since the d-axis of the reference frame is parallel with the stator flux space vector.

$$T_{em} = \frac{3}{2} p \frac{L_m}{L_s} (\psi_{qs} i_{dr} - \psi_{ds} i_{qr}) \tag{3.104}$$

$$T_{em} = -\frac{3}{2} \mathrm{p} \frac{L_m}{L_s} |\psi_s| i_{qr} \tag{3.105}$$

$$T_{em} = K_T i_{qr} \tag{3.106}$$

As seen in the expression rotor current component and the q component are inversely related. The ability to control torque via i_{qr} (machine speed control is also possible). In addition, Q_s control with d_q frame can be performed by i_{dr} by defining the reactive power for the stator.

$$Q_s = \frac{3}{2} (v_{qs} i_{ds} - v_{ds} i_{qs}) \tag{3.107}$$

$$Q_s = -\frac{3}{2} \omega_s \frac{L_m}{L_s} |\psi_s| \left(i_{dr-} \frac{|\psi_s|}{L_m} \right) \tag{3.108}$$

$$Q_s = K_Q \left(i_{dr-} \frac{|\psi_s|}{L_m} \right) \tag{3.109}$$

These methods reveal that it is feasible to do so independently control the reactive power and torque of the stator for the two rotor current components. The full vector control method for DFIG is indicated in the Figure 14. The reactive power of a stator loop

and speed loop is added to system while the current loop is preserved. Because the machine's electricity grid is directly connected to the stator, the voltage level determines the constant amplitude of the stator flow$|\psi_s| = |v_s|/\omega_s$ so the stator flux equation.

$$|\psi_s| = \psi_{ds} = L_s i_{ds} + L_m i_{dr} \tag{3.110}$$

$$|\psi_{qs}| = 0 = L_s i_{qs} + L_m i_{qr} \tag{3.111}$$

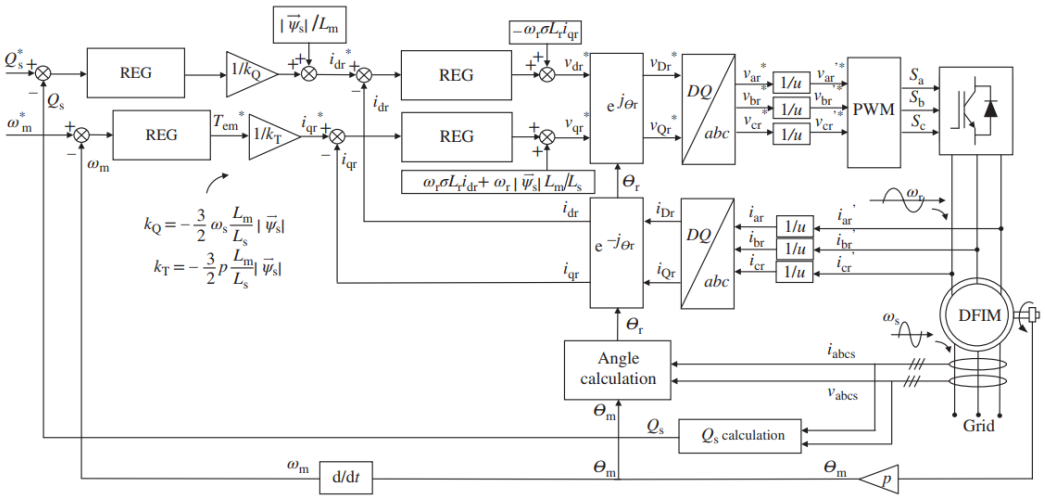

Figure 14. DFIM's full vector control

By preserving a certain quantity of grid backup power programmed into the wind turbine control support, the grid's frequency can be supplied by avoiding maximum wind power extraction and operating at different greater than ideal speeds. By using this technique, the wind farm helps the grid generate energy. It could be necessary for wind turbines to act inertia to frequency changes. In normal operation, wind turbines store kinetic energy in moving blades. By simulating an inertia response to the wind turbine, a fast torque is applied with proportional derivative control in a change in the frequency limit value. This situation also changes the electricity delivered to the grid. This is accomplished by altering the blades' rate of rotation and, as a result, the wind turbine's saved kinetic energy. With this quick reaction, abrupt frequency fluctuations induced by unexpected increases in power consumption perhaps prevented, and power plants can be shut down if overcoming the frequency deviation. The wind turbine will stop operating

at suboptimal speeds and contribute to the inertial response without drawing the most power possible from the wind when a certain level of rotational speed is reached (maximum or lowest). Provides increased power during the initial few minutes of frequency variation. The wind turbine runs against its base frequency setting and reaches its optimum speed again. Fast synchronization mechanisms such as Phase Locked Loop (PLL) are needed to provide fast and accurate information about frequency changes.

CHAPTER 4

RESULT AND DISCUSSION

In this part of the thesis, the Simulation process, which was created with Matlab / Simulink, will be explained, and the results will be shared.

4.1. Design of the Control of DFIG

The vector control approach is used to regulate the DFIG's rotor currents by overlapping the reference plane on the same axis with the flux relations as illustrated in Figure 14. In general vector control, stator-flux field or grid-flux routing methods are used. Considering that there is little stator resistance, stator-flux steering is also performed with stator voltages. The rotor currents are inversely proportional to the capabilities of the stator that are active and reactive because the synchronous reference plane coincides with the stator flux. As a result of this, the flow of power control involving the grid and the stator are realized by controlling the rotor currents. An RSC and a GSC include the two converters that constitute DFIG. With the control of the RSC, the active and reactive capabilities of the stator can be controlled independently, and the DC connection voltage is controlled by the GSC, which perhaps maintained independently of the rotor's power. Although normally in RSC control, GSC provides for the adjustment that is reactive power. As a result of RSC control the guarantee that the rotor frequency and tip voltages are kept within the desired level range. In DFIG, control is provided by a vector control algorithm in illustrated Figure 15. that controls rotor currents. In both planes of reference, the produced torque or the rotor current's q component determines active power, the d component, on the other hand, is utilized to manage the voltage at the stator terminals' reactive power. For rotor control, reference currents were determined first, and reference power values were obtained by using reference currents. It has been concluded that the connection between rotor currents and voltages is important for controlling Dfig.

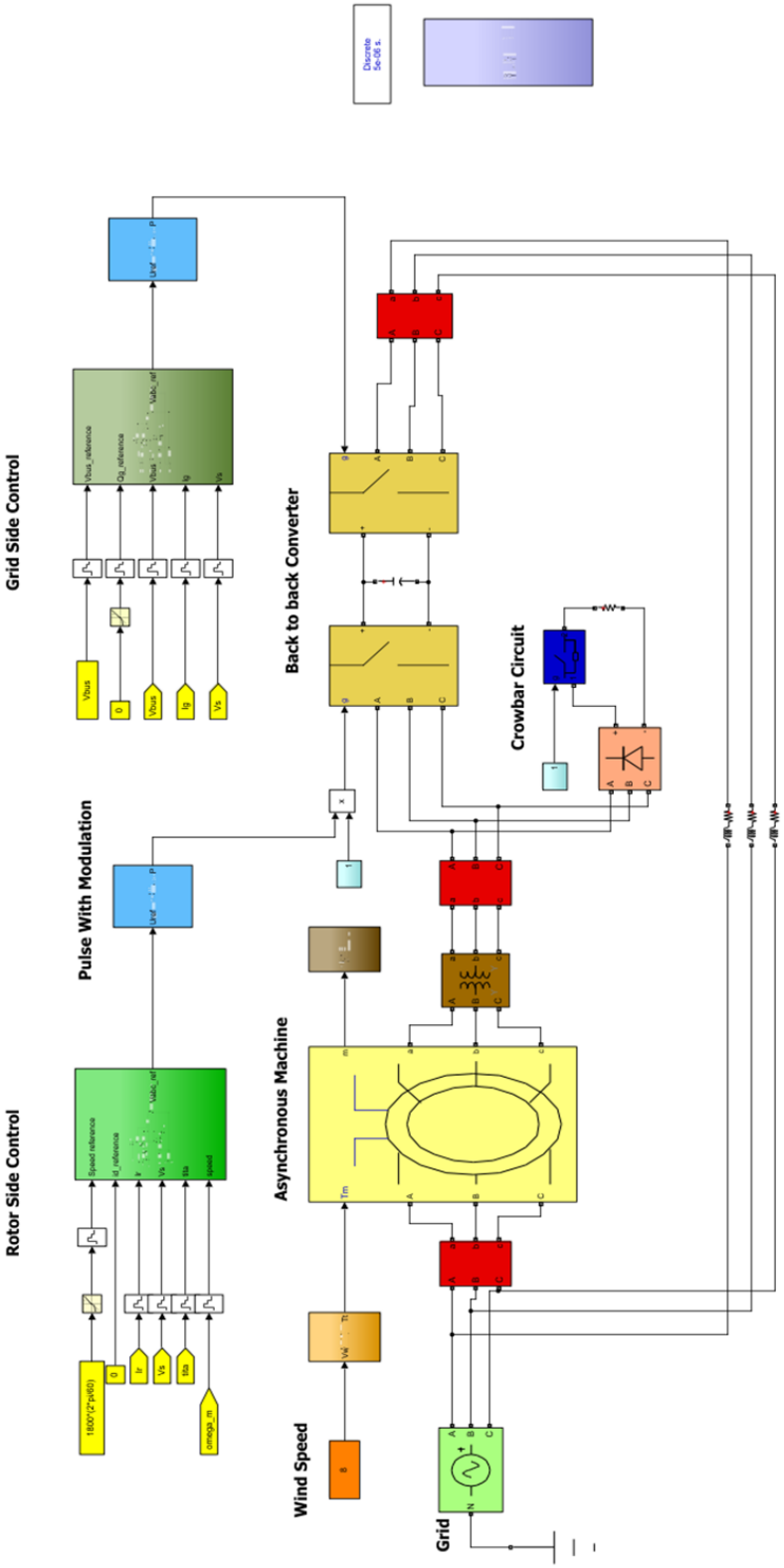

Figure 15. DFIG system with RSC and GSC control in Simulink

The back-to-back converter includes a common dc bus, RSC, and a GSC. As the power converter for the DFIG, an average AC/DC/AC converter model was used. Power converters frequently include the following features: power control, RSC dc-link dynamics, grid control, and current control. These converters need voltage to work. A DC-coupled capacitor uses strongly modified devices of power electronic. IGBTs function as a DC voltage source when they synthesise a DC voltage converted to AC voltage. With a coupling inductor L, GSC is connected to the grid. The stator is connected directly to the grid, while the rotor is connected to the grid via 3-phase slip rings. While the grid is unmistakably connected to the three-phase stator winding, RSC is connected to the three-phase rotor winding by slip rings and brushes. The wind turbine's generated power is transformed into electrical energy and powered by the windings on the rotor and stator and transmitted to the grid. The control system uses the voltage at the grid terminals and the DC bus voltage to adjust the wind turbine's power. For this, RSC and GSC create the pitch angle and voltage command signals Vr and Vgc. IGBT is used to get DC to AC voltage conversion source as converter components. The rotor and grid can produce or consume voltage regulation or reactive power at grid terminals are both possible uses for reactive power.

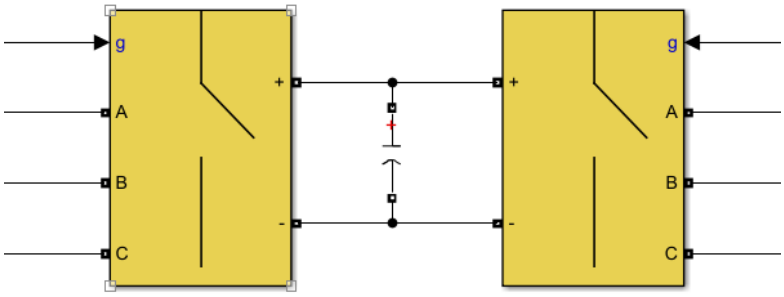

Figure 16. Converter for AC/DC/AC in Simulink model

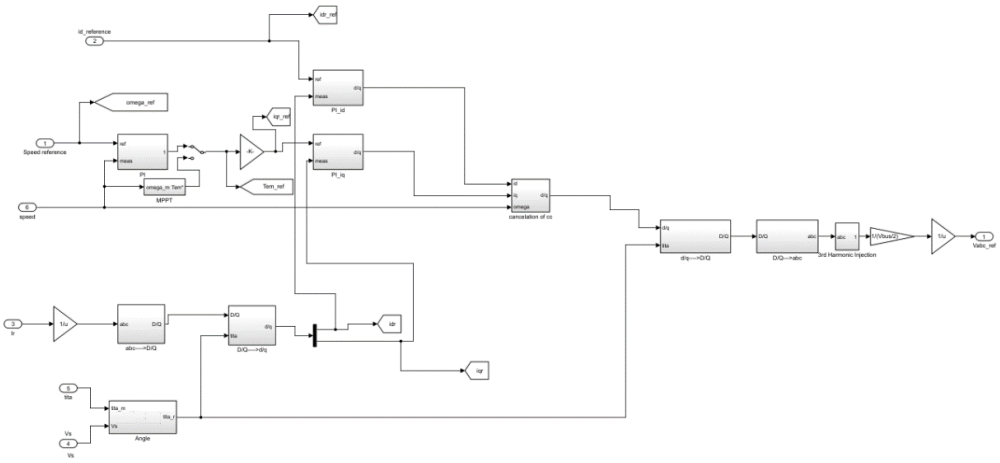

Figure 17. Control of RSC

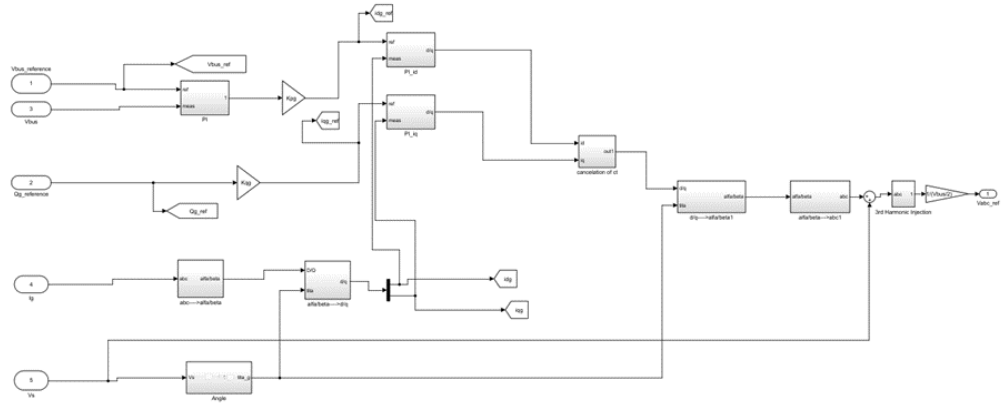

Figure 18. Control of GSC

In the Simulink model shown in Figure 14, one end of the 3-phase programmable voltage source is connected to the ground and the power required for the generator to operate is drawn from the grid. By adding a three-phase V-I measurement between the grid and the generator, voltage current values are observed in all cases. The GSC is fed directly by connecting to the grid. The GSC charges the DC connection on the RSC. The RSC regulates both active and reactive power and torque. The parameters for speed and torque are sent to the system. With these parameters coming derived from the RSC, flux originating from the rotor and the stator are separated by a magnetic field. With this flux, the DC limit of the converter is increased and when the on the grid side, a DC link starts to fill up, the current from the grid starts to flow in the opposite direction. With the DC

bus full, when the rotor speed of the doubly fed asynchronous machine starts to rotate faster than the synchronous speed, the machine starts to work in generator mode with reverse current. The turbine generates power for the grid. In DFIG, the magnetic flux produced by the rotor, stator windings, and the rotor is fed from the grid. Ig and Ir are controlled using a PWM converter. It is necessary to equalize the voltage frequency of the grid and the stator. By adjusting the frequency of the rotor fed with PWM converters, the stator frequency is maintained. Using PWM, the magnitude of the changing frequency of the voltage at the rotor terminals of the induction generator is converted into a direct current voltage. This process is speed independent and is one of the primary causes DFIG is used in variable speed applications. Converters control the output voltage after powering both active and reactive production to maintain the system running smoothly over a broad speed range. To protect the power converter, the crowbar circuit (reduces the load by ensuring that the power supply's output terminals are short-circuited when an overvoltage condition is recognized and integrated into the system, ensuring that the current reaches the desired level before reaching the power converter, thus protecting the power converter in case of sudden current changes) is used. In the simulation, the voltage problem was created at 3.s and when the crowbar was activated at 3.1 s, it was seen that all the energy flowed into the crowbar. Thus, the RSC is protected from sudden voltage changes. The explanations of all the block diagrams used in the Simulink model shown in Figure 15 are explained in the order below.

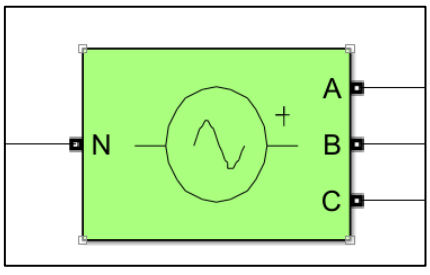

Figure 19. 3-phases programmable voltage source

A 3-phase programmable voltage source is used to obtain the power needed from the grids for the generator to operate.

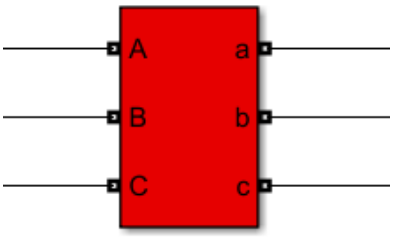

Figure 20. Three phase V-I measurement

For following the voltage levels during the system's working time, 3-phase V-I measurements are added between the grid and the generator to read the voltage current values.

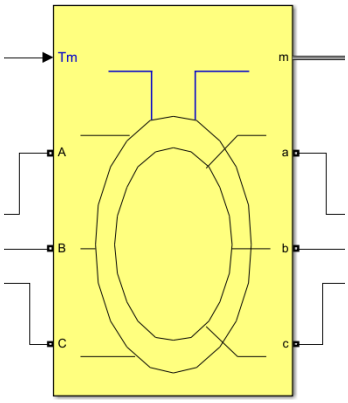

Figure 21. Asynchronous machine

The asynchronous machine, which consists of two main parts, a stator (stationary) and rotor (moving) and works as a generator in the system, is used in mechanical energy to electrical energy conversion.

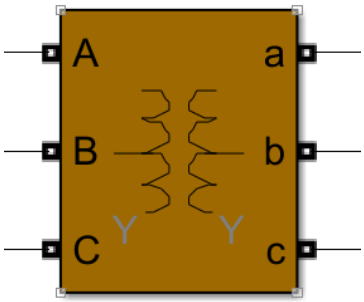

Figure 22. Three phase transformers

With a 3-phase transformer, it is possible to reduce and increase the alternating current (AC) and the voltage level at the required rate without changing the frequency by using electromagnetic induction to transfer energy from one circuit to the other.

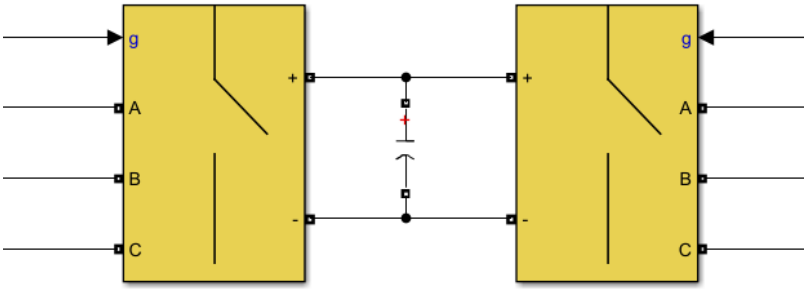

Figure 23. AC/DC/AC Back-to-back converter

The converter's grid side is also fed directly by connecting to the grid. The converter on the GSC charges the converter on the RSC and activates the DC link. Speed and torque are controlled by RSC and speed and torque parameters are sent to the system. With these parameters coming from the RSC, the flux originates the magnetic field that develops between the rotor and the stator. These current increases the DC limit of the converter when the DC connection is filling up and on the generator side on the grid's side, the current from the grid starts to flow in the opposite direction.

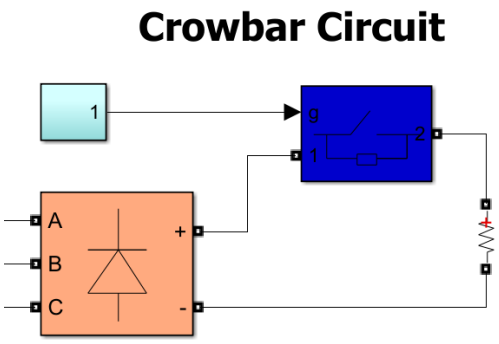

Figure 24. Crowbar circuit

In case of a power supply fault, sometimes the circuit powered by the power supply is damaged beyond repair. An electrical circuit called the Crowbar Circuit is that reduces the system's power supply's load to prevent damage to the circuits in the event of an overvoltage in the load supplied to the power source. The Crowbar Circuit detects an overvoltage when it occurs to decrease the load by shorting the power supply's output terminals. When the output terminals of the power supply are shorted, the high current flow causes the fuse to blow, thus disconnecting the power supply from the remainder of the circuit. In other words, the Crowbar circuit detects overvoltage and blows the fuse.

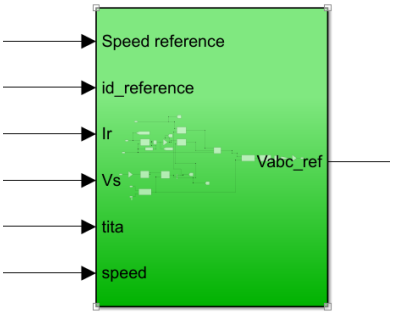

Figure 25. RSC control block

With the RSC, DFIG's torque, speed and power factor in the stator circuit can be controlled. The 3-phase voltage passing through the RSC control is regulated by entering the PWM. With the pulses produced in PWM, the inverter is kept constant to output at the desired voltage level.

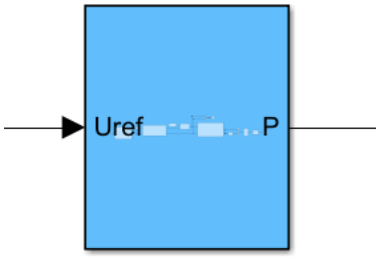

Figure 26. PWM block in Simulink

PWM is a method for achieving the required analogy electrical value or signals at the output by regulating the widths of the pulses to be produced. The analogy value to be created at the output is determined by the average of the widths of the generated square wave pulse signals. One of the most significant benefits of PWM is that it provides a very basic framework for the digital-to-analogy conversion process.

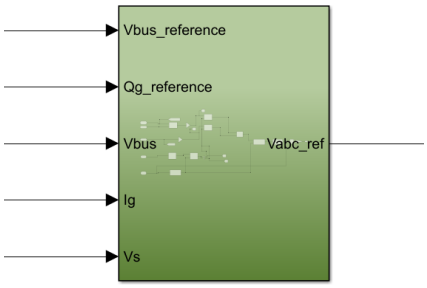

Figure 27. GSC block diagram

The GSC controller has two loops. The outer loop controls the reference i_d_ref current. The internal loop controls and keeps the DC link voltage constant. Manages the outer loop as a PI controller. The outer loop scales the output voltage level and compares it to the provided reference to generate the error that serves as the input for the PI controller.

4.2. Simulation

Firstly, the simulation results are shown for the rotor and grid sides, and then the voltage problem and the results in the rotor, grid, and crowbar circuit at the fault are shown.

4.2.1. Simulation Scenario

Table 2. Shows input parameters in the simulation are given.

Stator frequency (Hz)	f= 50
Rated stator power (W)	Ps = 26000000
Rated rotational speed (rev/min)	n = 1680
Rated stator voltage(V)	Vs = 690
Rated stator current(A)	Is = 1973,5
Rated torque (N. m)	Tem = 15047
Pole pair	p=2
Stator rotor current turns ratio	u = 1/3
Rated rotor voltage (V)	Vr = 2070
Max slip	smax = 1/3
Rated rotor voltage referred to the stator(V)	Vr_stator = (Vr*smax) *u
Stator resistance (ohm)	Rs = 2.6e-3
Leakage inductance (stator-rotor) (H)	Lsi = 0.087e-3
Magnetizing inductance (H)	Lm = 2.5e-3
Rotor resistance referred to stator(ohm)	Rr = 2.9e-3
Stator inductance(H)	Ls=Lm + Lsi
Rotor inductance(H)	Lr=Lm + Lsi
DC bus voltage referred to the stator(V)	Vbus = 1150
Stator flux (Wb)	Fs=Vs*sqrt(2/3)/(2*pi*f)
Inertia	J = 127/2

4.2.2. Simulation Results

The simulation results in presented in this section and will be shared under 3 topics: RSC, GSC, and Crowbar circuit.

4.2.2.1. Simulation Results of RSC

A simulation study was conducted to examine the energy transfer to the grid of a 2.6 MW wind turbine with a variable-speed doubly fed induction generator (DFIG) under an 8.5 m/s wind speed. The simulation study was initiated with the turbine rotor speed at zero. The machine is directly connected to the grid, and the perturbation is strong. The speed has increased gradually. The Figure 28 illustrate the responses of the parameters evaluated on the rotor-side converter in the simulation.

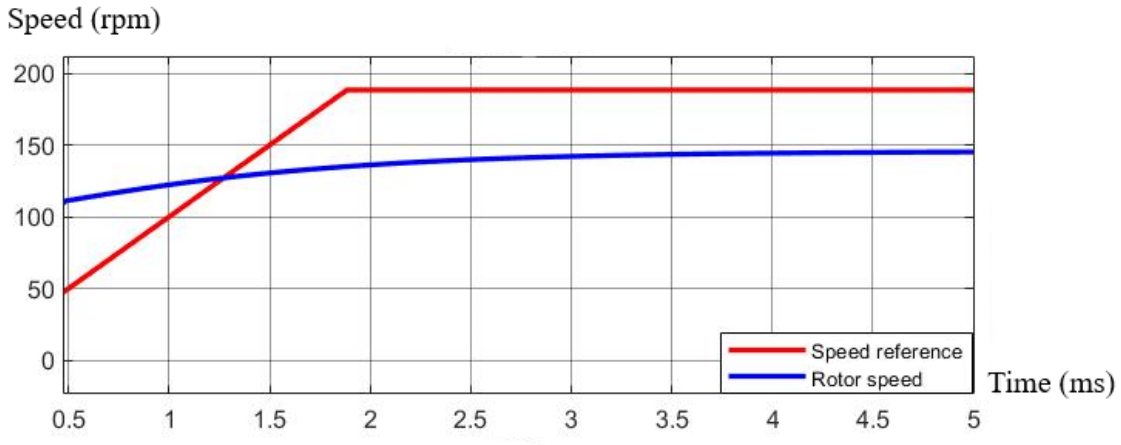

Figure 28. Rotor speed value for DFIG based wind turbine

The rotor speed was defined as 188.5 rpm. When the induction machine started to rotate faster than the synchronous speed, it started to work as a generator and the rotor speed remained constant.

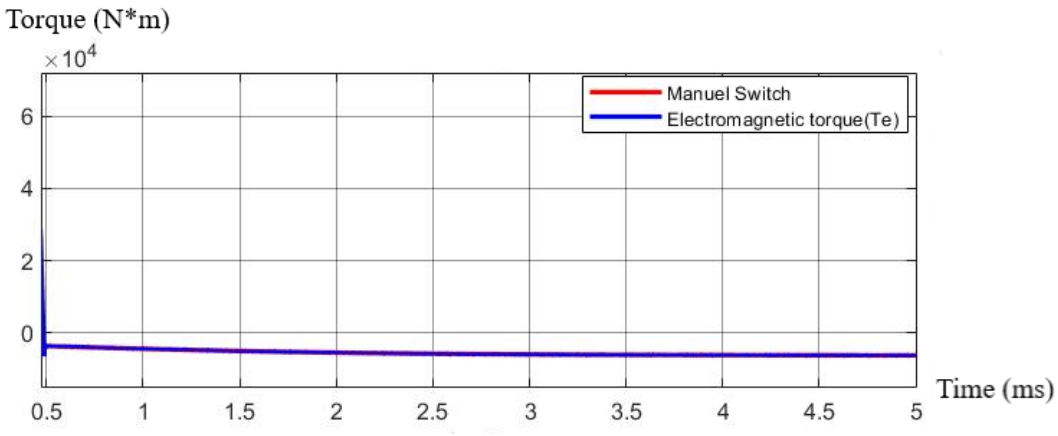

Figure 29. Rotor speed value for DFIG based wind turbine

Similarly, the torque-speed is increased first and then remained at a steady state (within ± value range).

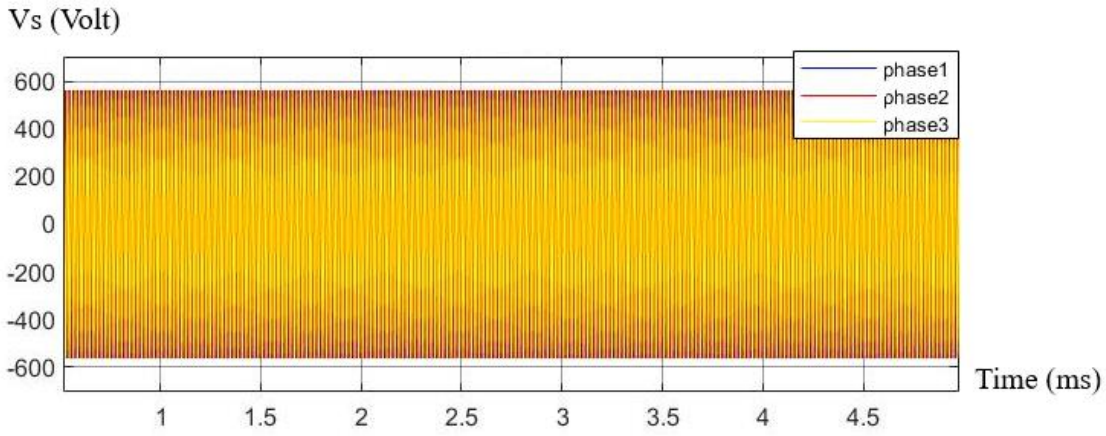

Figure 30. Stator voltage

The stator voltage is input as 690 into the system. In the simulation, the stator voltage changes sinusoidally between ± 560.

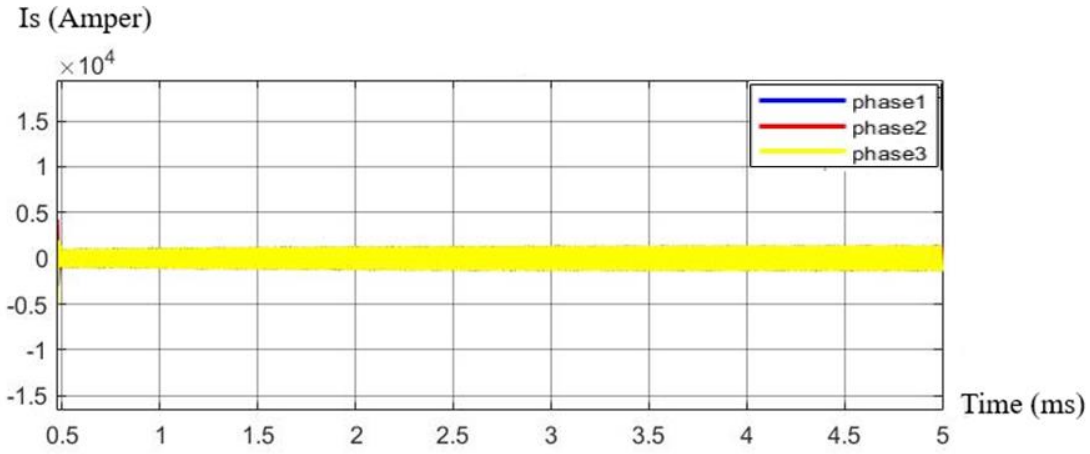

Figure 31. Stator current

The stator's current reference value input to the system is 1973.5 and the current showed a change in accordance with the reference value.

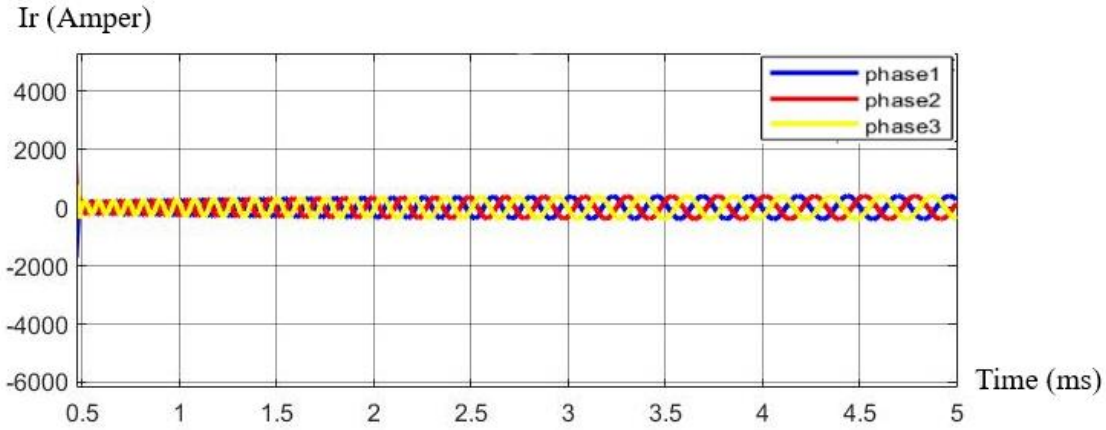

Figure 32. Rotor current

It is seen that 3-phase rotor current is in steady state after generator operation. Rotor current values were analysed for various wind speeds.

4.2.2.2. Simulation outputs of GSC

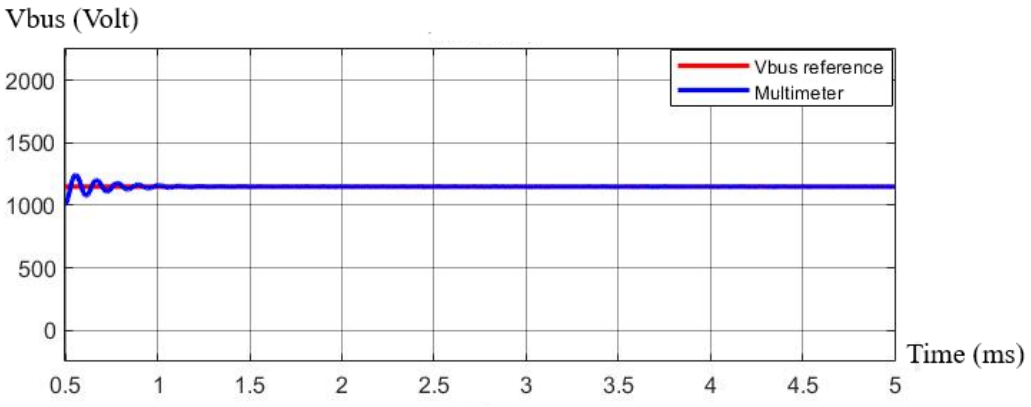

Figure 33. Bus voltage

The busbar voltage increased starting from zero and increased to approximately 2000 V with the charging of the busbar capacitor. DC bus voltage is kept constant with grid side converter control.

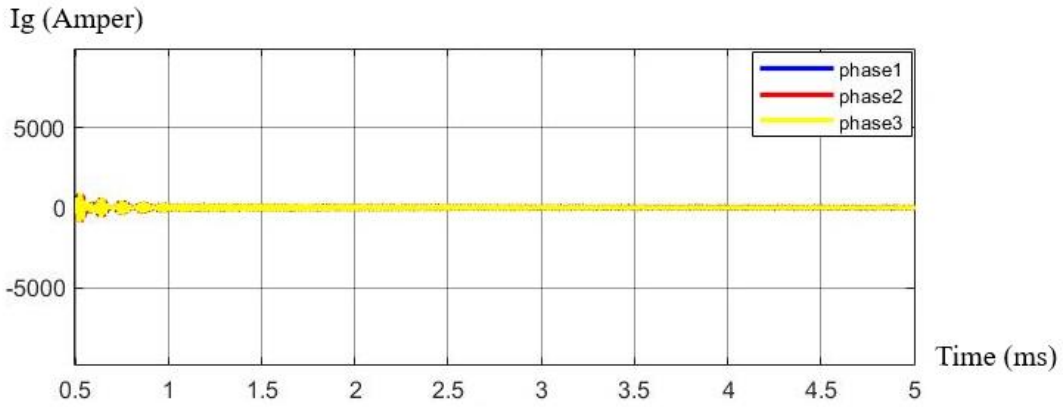

Figure 34. The grid side current

The grid current is stable after operation in generator mode.

4.2.2.3. Crowbar control

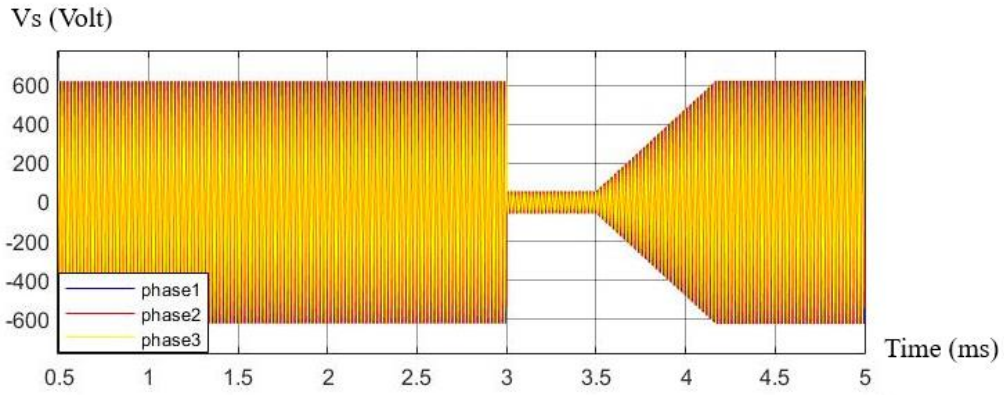

Figure 35. The Stator voltage

A voltage drop was created in the system in the 3rd second, and the crowbar system was activated in 3.1 s, and it was seen that the system recovered, and the stator voltage recovered to its normal range in the range of 3.5-4.17 s.

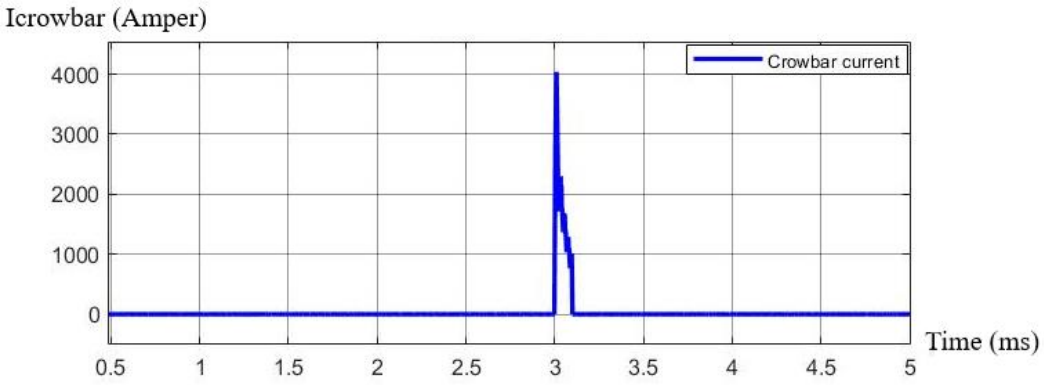

Figure 36. Crowbar current

It has been shown that the crowbar system works with the sudden increase in the crowbar current in 3-3.1 s, which is the fault moment, by opening the switch to which the crowbar circuit is connected, only at the time of the fault.

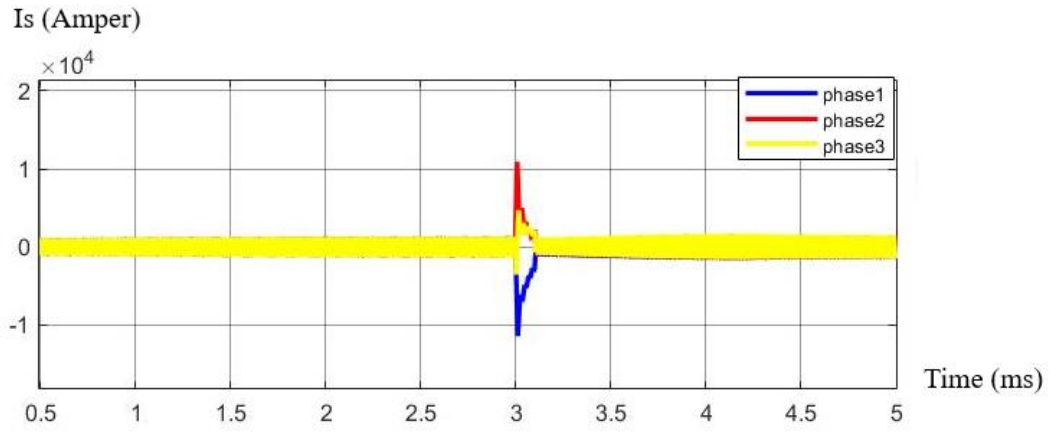

Figure 37. Stator current

The stator current is stable during the whole operation of the system and the change during the fault moment is shown. It is seen that the stator current returns to a steady state with the activation of the crowbar system.

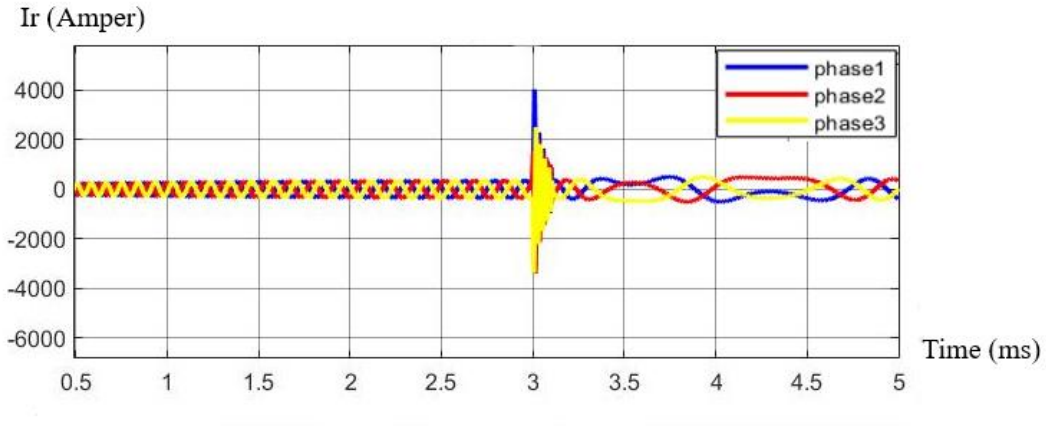

Figure 38. Rotor current

The rotor current is stable during the whole operation of the system and the change during the fault is shown. It is seen that the rotor current returns to a steady state with the activation of the crowbar system.

4.3. Analysis of Symmetric faults with the Monte Carlo Method

The thesis work was completed in three parts. In the first part, the vector control method was applied with Park and Clarke transformations, and active power, reactive power, torque, and DC link control were provided for the back-to-back converter. It was seen that the model parameters simulated with Matlab / Simulink were in a steady state.

In the second part, after testing that the system works properly with rotor and grid-side converter control and no abnormality (a sudden decrease or increase) in the simulation results was observed, the voltage dip was manually created on the system by multiplying the stator voltage by a factor of 0.1. In the voltage deep created, the fault was activated in the 3rd second. In the second part, the crowbar is activated, and the current and voltage drop are taken under control. It has been observed that the sudden increase and decrease in the crowbar also reduces the flux. Since all the current is collected on the crowbar, the RSC is protected.

In the last part, stator voltage (Vs) and rotor current (Ir) values were observed by creating 20 different voltage drops at 8.5 m/s wind speed with Simulink. For Vs and Ir, a total of 4 separate parameters were evaluated for the time in steady state and when the system entered an fault. The mean and standard deviation values for these parameters were calculated for 20 different samples using the normal distribution function with the help of Excel. Then normal distribution graphs were drawn. With these values, 1000 random samples were selected in Excel and 1000 steady state and fault values of Vs, Ir were calculated. First, the average of these values was taken to calculate the percentage increase in the rotor current that the decrease in stator voltage would cause. Then, the percentage change ranges of the rotor current depending on the fault in the stator voltage were determined.

4.3.1. Monte Carlo Method

Monte Carlo simulation is a group of numerical computation techniques that are widely used in many sectors of research to get numerical findings through a large number of repeated random samples. It is extremely beneficial for forecasting the outcomes of physical processes involving stochastic occurrences and is also used to address a variety of deterministic issues when random options work. The fundamental notion of Monte Carlo simulation is ergodicity, which defines the statistical behavior of a moving point in a closed system. moving point will eventually pass through every potential location. This becomes the fundamental component of the Monte Carlo simulation, and the computer conducts enough simulations to generate the outcome of the many inputs. The fundamental notion of Monte Carlo simulation is ergodicity, which defines the statistical behaviour of a moving point in a closed system. moving point will eventually pass through every potential location. This becomes the fundamental component of the Monte Carlo simulation, and the computer conducts enough simulations to generate the outcome of the many inputs (Harrison and Robert L,2010).

Stator voltage (Vs) and rotor current (Ir) values were observed by creating 20 different voltage drops at 8.5 m/s wind speed with Simulink. For Vs and Ir, a total of 4 separate parameters were evaluated for the time in steady state and when the system entered a fault. The mean and standard deviation values for these parameters were calculated for 20 different samples using the normal distribution function with the help of Excel and the results are shared in Table 3.

Table 3. Shows the Vs, and Ir values before and after the faults.

	Steady state		During the fault	
Wind Speed (Ws) (m/s)	Stator Voltage (Vs) (Volt)	Rotor current (Ir) (Amper)	Stator Voltage (Vs) (Volt)	Rotor Current (Ir) (Amper)
8.5	0.00068	0.00006	0.00057	0.04848
	0.00084	0.00008	0.00077	0.04870
	0.00106	0.00025	0.00100	0.02899
	0.00130	0.00055	0.00127	0.02053
	0.00155	0.00052	0.00155	0.02939
	0.00179	0.00046	0.00184	0.01458
	0.00200	0.00044	0.00218	0.02464
	0.00219	0.00020	0.00234	0.02129
	0.00232	0.00055	0.00249	0.05078
	0.00238	0.00055	0.00258	0.04145
	0.00239	0.00023	0.00258	0.04184
	0.00229	0.00049	0.00250	0.04320
	0.00219	0.00049	0.00234	0.01915
	0.00201	0.00050	0.00212	0.05090
	0.00180	0.00051	0.00182	0.02863
	0.00156	0.00056	0.00157	0.02430
	0.00131	0.00037	0.00129	0.02021
	0.00108	0.00055	0.00102	0.05141
	0.00085	0.00040	0.00078	0.03019
	0.00066	0.00024	0.00058	0.04753

Normal distribution graphs for the Vs and Ir parameters are given below.

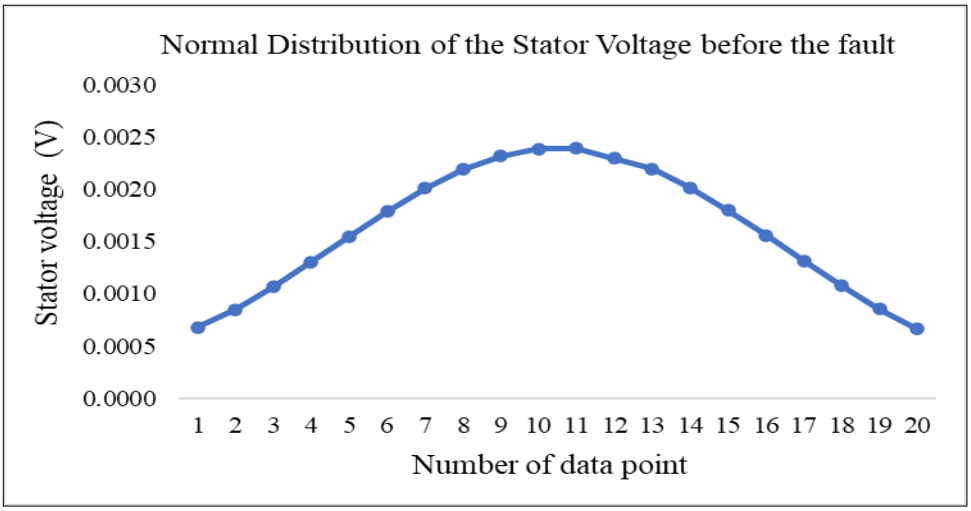

Figure 39. Normal distribution of the Stator Voltage before fault

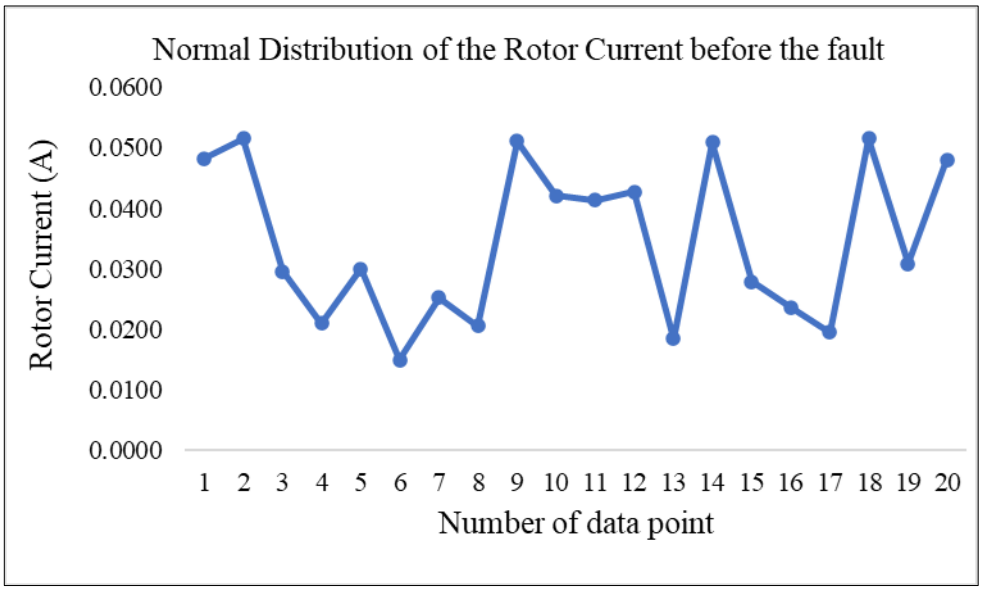

Figure 40. Normal distribution of the Rotor current before fault

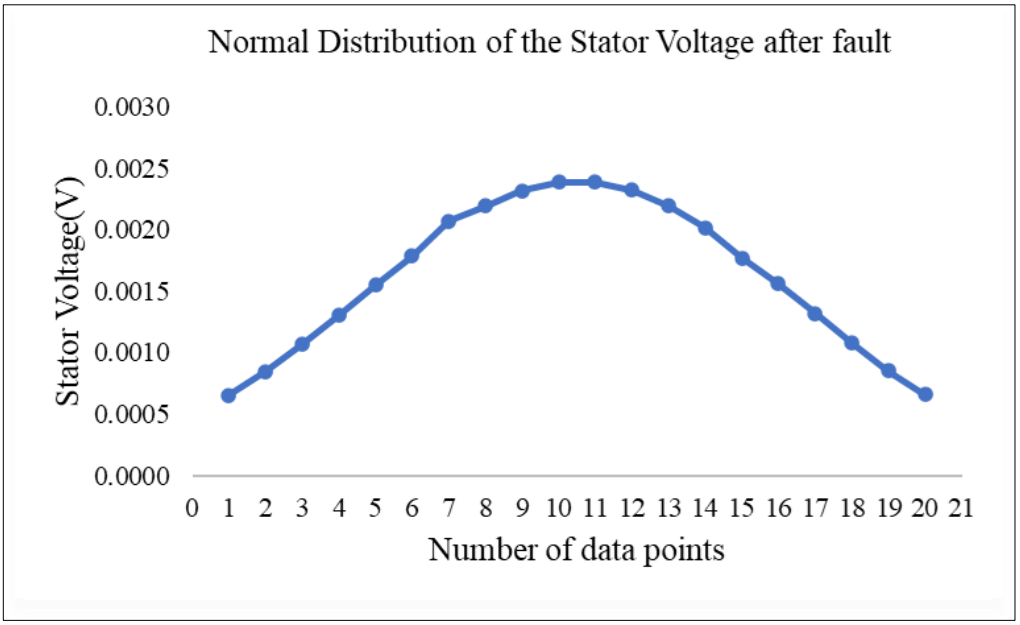

Figure 41. Normal distribution of the Stator Voltage after fault

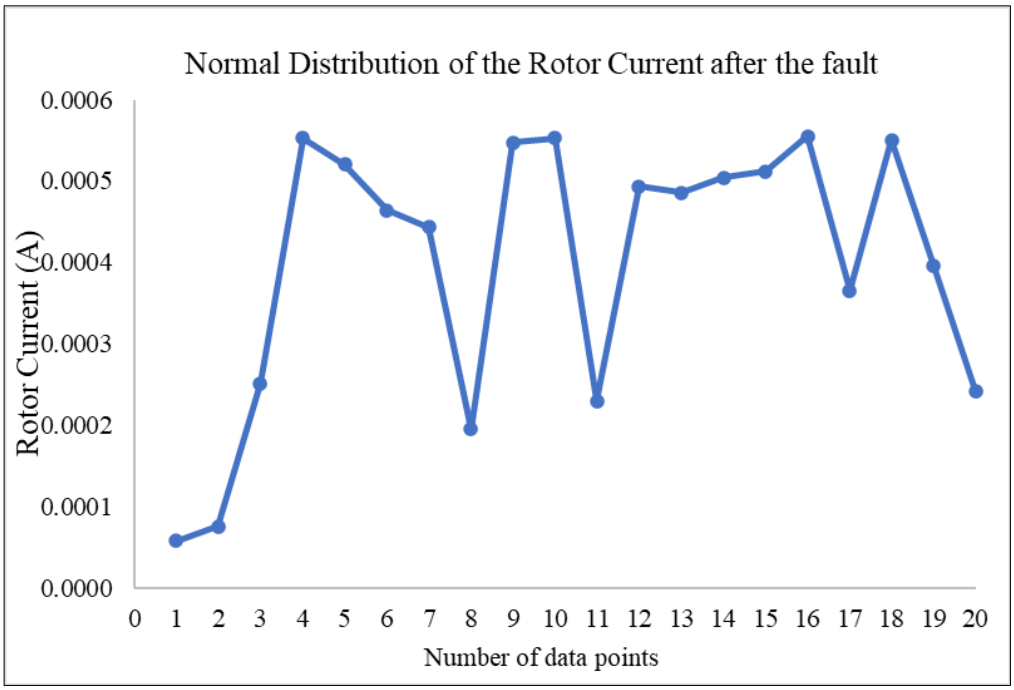

Figure 42. Normal distribution of the Rotor current after fault

Table 4. Shows the Vs and Ir mean and standard deviation values before and after the fault

	Steady state		**During the fault**	
	Stator Voltage (Vs) (Volt)	Rotor current (Ir) (Amper)	Stator Voltage (Vs) (Volt)	Rotor current (Ir) (Amper)
Mean	679.7	296.3	292.3	2472.3
Standard deviation	93.3	166.4	7.6	718.4

With Table 4, 1000 random numbers were generated, and 1000 values were predicted for the stator current and rotor current.

With these values, 1000 random samples were selected in Excel and 1000 steady state and fault values of Vs, Ir were calculated, and the results are shown in Table 5.

Table 5. Shows the values which calculated with 1000 random values for the average and standard values of stator voltage and rotor current.

Simulation Step	Random Values	Vs (V)	Vs (V) under the fault	Ir (A)	Ir (A) under the fault
1	0.496	678.8	268.2	292.2	2465.9
2	0.798	757.5	320.2	298.6	3071.4
3	0.375	649.8	-34.8	289.9	2242.7
4	0.784	753.0	222.8	298.3	3036.4
5	0.638	712.7	195.0	295.0	2726.2
6	0.522	684.9	340.8	292.7	2512.6
7	0.642	713.6	291.0	295.1	2733.3
8	0.364	647.2	45.1	289.7	2222.4
9	0.089	554.2	608.4	282.1	1506.4
10	0.037	512.8	71.7	278.8	1187.4
.	.	.	.	.	.
.	.	.	.	.	.
.	.	.	.	.	.
1000	0.513	470.5	76.2	292.6	2495.3

Changes in stator voltage and rotor current for possible values obtained with Monte Carlo are shown in the Table 6.

Table 6. Shows the percentage change of Vs and Ir.

ΔVs (%)	**ΔIr (%)**
-57	744
-43	929
-63	674
-43	918
-50	824
-55	758
-50	826
-63	667
-87	434
-100	326
.	.
.	.
.	.
-56	753

The average of these values was taken to calculate the percentage increase in the rotor current that the decrease in stator voltage would cause. and the results are shown in Table 7.

Table 7. Shows the average percentage change of Vs and Ir.

Average	
ΔVs (%)	**ΔIr (%)**
-59	740

In the Table 8, the percentage change ranges of the rotor current depending on the fault in the stator voltage were determined.

Table 8. Shows the percentage change ranges of the rotor current depending on the fault in the stator voltage were determined.

ΔVs- (%)	**ΔIr+ (%)**
0-10	0.0
10-20	1388.3
20-30	1192.7
30-40	1028.8
40-50	893.5
50-60	769.4
60-70	649.5
70-80	541.9
80-90	459.3
90-100	369.9

As a results of the symmetric faults analysis, it was observed that sudden peak values occurred in the rotor current after the voltage drop. As the symmetric fault percentages increased, these sudden peaks in the rotor current decreased. A symmetric fault causes the stator and rotor flux values to decrease. These changing flux and voltage values in the generator cause high instantaneous currents to flow through the stator and rotor windings. The rotor current can reach very high instantaneous values, which can damage the power electronic circuits in the converter. With the Crowbar method, in cases where the rotor current is high or the DC-link voltage exceeds the limit value, the rotor of the generator is short-circuited through power electronic switches and external resistors. This method protects the converter system and ensures that the turbine remains connected to the grid.

CHAPTER 5

CONCLUSION

In this thesis, the simulation of the double-fed asynchronous generator system, which is one of the wind energy conversion technologies, was carried out. For this purpose, a wind turbine with a nominal power of 2.6 MW was modelled and controlled. First, with the Clarke and Park transformation techniques, the natural reference frame abc was derived and a comprehensive dynamic model of DFIG was developed in a rotating reference frame dq. Then, the wind speed model, aerodynamic model, and electrical model were developed in the MATLAB/Simulink environment with the help of data provided by the literature and manufacturers. Two different control algorithms were created for GSC and RSC, and it was observed that dfig controls torque and power at 8.5 m/s wind speed. Stator voltage, grid, and rotor current parameters, which are important in the integration of the system with the grid, were examined in steady state.

Based on the principle that WECSs connected to the grid must contribute to the grid by maintaining system stability during a fault, in the second part of the study, a fault was applied to the stator voltage, and the change in the rotor current in the event of a sudden voltage drop and a possible drop in the stator voltage was examined. To solve the fault, the crowbar circuit has been added to the system. It was observed that when the crowbar circuit was activated during the drop in stator voltage, the system recovered and continued to contribute to the grid.

In the last part of the thesis, to analyse the effect of the symmetrical fault on the rotor current, the steady state and fault values were taken for the stator voltage and the rotor current by creating different voltage drops in the simulation in different voltage drop scenarios obtained with Simulink. The mean and standard deviation values for these parameters were calculated for 20 different samples using the normal distribution function with the help of Excel. With these results, 1000 possible Vs and Ir values were created using the Monte Carlo method for 1000 random samples. For these 1000 samples, it was calculated how much of a percentage decrease in stator voltage caused a percentage increase in the rotor current. These percentage decreases were averaged for 1000 samples.

Additionally, the ranges of percentage decreases in the stator voltage were determined, and their equivalents in the rotor current were calculated. Thus, by investigating the effect of a possible voltage drop on the rotor current, the behaviour of a DFIG-based wind turbine in the event of a possible fault can be predicted. By predetermining the response of the system in case of fault, the necessary protection circuits are added to the system, allowing WECS to continue contributing to the grid by maintaining system stability in the event of a possible fault.

REFERENCES

Abu-Rub, Haitham, Atif Iqbal, and Jaroslaw Guzinski. *High performance control of AC drives with Matlab/Simulink*. John Wiley & Sons, 2021.

Ackermann, Thomas, ed. *Wind power in power systems*. John Wiley & Sons, 2012.

Altın, Müfit, et al. "Overview of recent grid codes for wind power integration." *2010 12th international conference on optimization of electrical and electronic equipment*. IEEE, 2010.

Babu, B. Chitti, and K. B. Mohanty. "Doubly-fed induction generator for variable speed wind energy conversion systems-modeling & simulation." *International journal of computer and electrical engineering* 2.1 (2010): 141.

Beltran, Brice, Mohamed El Hachemi Benbouzid, and Tarek Ahmed-Ali. "Second-order sliding mode control of a doubly fed induction generator driven wind turbine." *IEEE Transactions on Energy Conversion* 27.2 (2012): 261-269.

Blaabjerg, Frede, et al. "Overview of control and grid synchronization for distributed power generation systems." *IEEE Transactions on industrial electronics* 53.5 (2006): 1398-1409.

Bongiorno, Massimo, and Torbjörn Thiringer. "A generic DFIG model for voltage dip ride-through analysis." *IEEE Transactions On energy conversion* 28.1 (2013): 76-85.

Brekken, Ted, Ned Mohan, and Tore Undeland. "Control of a doubly-fed induction wind generator under unbalanced grid voltage conditions." *2005 European conference on power electronics and applications*. IEEE, 2005.

Burton, Tony, et al. *Wind energy handbook*. John Wiley & Sons, 2011.

Byeon, Gil-Sung, In-Kwon Park, and Gil-Soo Jang. "Modeling and control of a doubly-fed induction generator (DFIG) wind power generation system for real-time simulations." *Journal of Electrical Engineering and Technology* 5.1 (2010): 61-69.

Code, Transmission. "Network and system rules of the German transmission system operators." *VDN-ev beim VDEW* (2007).

Coşkun, İsmail, Ali Saygın, and Mahir Dursun. “Matris Konverter Uygulaması.” *Politeknik Dergisi* 11.3 (2008): 193-198.

Dufour, Christian, and Jean Belanger. “A real-time simulator for doubly fed induction generator based wind turbine applications.” *2004 IEEE 35th Annual Power Electronics Specialists Conference (IEEE Cat. No. 04CH37551)*. Vol. 5. IEEE, 2004.

Ekanayake, Janaka B., et al. “Dynamic modeling of doubly fed induction generator wind turbines.” *IEEE transactions on power systems* 18.2 (2003): 803-809.

Ekanayake, Janaka Bandara, L. Holdsworth, and Nick Jenkins. “Comparison of 5th order and 3rd order machine models for doubly fed induction generator (DFIG) wind turbines.” *Electric Power Systems Research* 67.3 (2003): 207-215.

Etxeberria-Otadui, Ion, et al. “New optimized PWM VSC control structures and strategies under unbalanced voltage transients.” *IEEE Transactions on Industrial Electronics* 54.5

Fadaeinedjad, Roohollah, Mehrdad Moallem, and Gerry Moschopoulos. “Simulation of a wind turbine with doubly fed induction generator by FAST and Simulink.” *IEEE Transactions on energy conversion* 23.2 (2008): 690-700.

Flannery, Patrick S., and Giri Venkataramanan. “A fault tolerant doubly fed induction generator wind turbine using a parallel grid side rectifier and series grid side converter.” *IEEE Transactions on power electronics* 23.3 (2008): 1126-1135.

Gagnon, Richard, et al. “Modeling and real-time simulation of a doubly-fed induction generator driven by a wind turbine.” *Intl. Conference on Power Systems Transients, Canada*. 2005.

Hansen, Anca D., and Gabriele Michalke. “Fault ride-through capability of DFIG wind turbines.” *Renewable energy* 32.9 (2007): 1594-1610.

Hansen, Lars Henrik, et al. “Conceptual survey of generators and power electronics for wind turbines.” (2001).

Harrison, Robert L. “Introduction to monte carlo simulation.” *AIP conference proceedings*. Vol. 1204. No. 1. American Institute of Physics, 2010.

IEC 61400-12-1. “Wind turbines generator systems - Part 21: Power performance measurements of electricity producing wind turbines”, 2021.

Islam, Md Rabiul, Youguang Guo, and Jianguo Zhu. “Power converters for wind turbines: Current and future development.” *Materials and processes for energy: communicating current research and technological developments* (2013): 559-571.

Karaagac, Ulas, et al. “A generic EMT-type model for wind parks with permanent magnet synchronous generator full size converter wind turbines.” *IEEE Power and Energy Technology Systems Journal* 6.3 (2019): 131-141.

Karimi, Shahram, et al. “FPGA-based real-time power converter failure diagnosis for wind energy conversion systems.” *IEEE transactions on industrial electronics* 55.12 (2008): 4299-4308.

Krause, Paul C., et al. *Analysis of electric machinery and drive systems*. Vol. 2. New York: IEEE press, 2002.

Lei, Yazhou, et al. “Modeling of the wind turbine with a doubly fed induction generator for grid integration studies.” *IEEE transactions on energy conversion* 21.1 (2006): 257-264.

Li, Shuhui, and Ling Xu. “PWM converter control for grid integration of wind turbines with enhanced power quality.” *2008 34th Annual Conference of IEEE Industrial*

Lima, Francisco KA, et al. “Rotor voltage dynamics in the doubly fed induction generator during grid faults.” *IEEE Transactions on power electronics* 25.1 (2009): 118-130.

Lopez, Jesus, et al. “Dynamic behavior of the doubly fed induction generator during three-phase voltage dips.” *IEEE Transactions on Energy conversion* 22.3 (2007): 709-717.

Mei, Francoise, and Bikash Pal. “Modal analysis of grid-connected doubly fed induction generators.” *IEEE transactions on energy conversion* 22.3 (2007): 728-736.

Melício, R., V. M. F. Mendes, and João Paulo da Silva Catalão. “Power converter topologies for wind energy conversion systems: Integrated modeling, control strategy and performance simulation.” *Renewable Energy* 35.10 (2010): 2165-2174.

Morren, Johan, and Sjoerd WH De Haan. “Short-circuit current of wind turbines with doubly fed induction generator.” *IEEE Transactions on Energy conversion* 22.1 (2007): 174-180.

Muller, Set, M. Deicke, and Rik W. De Doncker. “Doubly fed induction generator systems for wind turbines.” *IEEE Industry applications magazine* 8.3 (2002): 26-33.

Netz, E. O. N. “Grid code—High and extra high voltage. E. ON Netz GmbH.” *Tech. Rep* (2006).

Pannell, Graham, David J. Atkinson, and Bashar Zahawi. “Minimum-threshold crowbar for a fault-ride-through grid-code-compliant DFIG wind turbine.” *IEEE Transactions on*

Park, Park Inverse. “Park, Inverse Park and Clarke, Inverse Clarke Transformations MSS Software Implementations User Guide.” 5-9.

Patel, Mukund R., and Omid Beik. *Wind and solar power systems: design, analysis, and operation*. CRC press, 2021.

Petersson, Andreas, et al. “Modeling and experimental verification of grid interaction of a DFIG wind turbine.” *IEEE Transactions on Energy Conversion* 20.4 (2005): 878-886.

Ramtharan, G., Nick Jenkins, and J. B. Ekanayake. “Frequency support from doubly fed induction generator wind turbines.” *IET Renewable Power Generation* 1.1 (2007): 3-9.

Rouco, L., et al. “Recent evolution of European grid code requirements and its impact on turbogenerator design.” *2012 IEEE Power and Energy Society General Meeting*. IEEE, 2012.

Saini, Shilpi. “Review of Doubly Fed Induction Generator Used in Wind Power Generation.” *International Journal of Environmental Science: Development and Monitoring* 4.3 (2013): 53-56.

Shariatpanah, Hamid, Roohollah Fadaeinedjad, and Masood Rashidinejad. “A new model for PMSG-based wind turbine with yaw control.” *IEEE transactions on energy*

Shi, Libao, et al. “Transient stability of power systems with high penetration of DFIG based wind farms.” *2009 IEEE Power & Energy Society General Meeting*. IEEE, 2009.

Slootweg, J. G., Henk Polinder, and Wil L. Kling. “Dynamic modelling of a wind turbine with doubly fed induction generator.” *2001 Power engineering society summer meeting. Conference proceedings (Cat. No. 01CH37262)*. Vol. 1. IEEE, 2001.

Stankovic, Ana Vladan, and Thomas A. Lipo. “A novel control method for input output harmonic elimination of the PWM boost type rectifier under unbalanced operating conditions.” *IEEE Transactions on Power Electronics* 16.5 (2001): 603-611.

Sun, Tao, Zhe Chen, and Frede Blaabjerg. “Flicker study on variable speed wind turbines with doubly fed induction generators.” *IEEE Transactions on Energy Conversion* 20.4 (2005): 896-905.

Takaai, Hitoshi, et al. “Pitch angle control of wind turbine generator using less conservative robust control.” *Transactions of the Society of Instrument and Control Engineers* 46.8 (2010): 486-492.

Thiringer, Torbjom, Andreas Petersson, and Tomas Petru. “Grid disturbance response of wind turbines equipped with induction generator and doubly-fed induction generator.” *2003 IEEE Power Engineering Society General Meeting (IEEE Cat. No. 03CH37491)*. Vol. 3. IEEE, 2003.

Wessels, Christian, Fabian Gebhardt, and Friedrich Wilhelm Fuchs. “Fault ride-through of a DFIG wind turbine using a dynamic voltage restorer during symmetrical and asymmetrical grid faults.” *IEEE Transactions on power electronics* 26.3 (2010): 807-815.

Xiang, Dawei, et al. “Control of a doubly fed induction generator in a wind turbine during grid fault ride-through.” *IEEE transactions on energy conversion* 21.3 (2006): 652-662.

Yazdani, Amirnaser, and Reza Iravani. *Voltage-sourced converters in power systems: modeling, control, and applications*. John Wiley & Sons, 2010.

Zou, Yu, Malik E. Elbuluk, and Yilmaz Sozer. “Simulation comparisons and implementation of induction generator wind power systems.” *IEEE Transactions on industry applications* 49.3 (2013): 1119-1128.

Zoubir, Zeghdi, Barazane Linda, and Larabi Abdelkader. “Field Oriented Control of Doubly Fed Induction Generator Integrated in Wind Energy Conversion System Using Artificial Neural Networks.” *2018 International Conference on Electrical Sciences and Technologies in Maghreb (CISTEM)*. IEEE, 2018.